Forces acting on a small particle in an acoustical field in a thermoviscous fluid

Karlsen, Jonas Tobias; Bruus, Henrik

Published in:
Physical Review E

Link to article, DOI:
10.1103/physreve.92.043010

Publication date:
2015

Document Version
Publisher's PDF, also known as Version of record

PHYSICAL REVIEW E **92**, 043010 (2015)

Forces acting on a small particle in an acoustical field in a thermoviscous fluid

Jonas T. Karlsen* and Henrik Bruus†

Department of Physics, Technical University of Denmark, DTU Physics Building 309, DK-2800 Kongens Lyngby, Denmark

(Received 3 July 2015; published 12 October 2015)

We present a theoretical analysis of the acoustic radiation force on a single small spherical particle, either a thermoviscous fluid droplet or a thermoelastic solid particle, suspended in a viscous and heat-conducting fluid medium. Within the perturbation assumptions, our analysis places no restrictions on the length scales of the viscous and thermal boundary-layer thicknesses δ_s and δ_t relative to the particle radius a, but it assumes the particle to be small in comparison to the acoustic wavelength λ. This is the limit relevant to scattering of ultrasound waves from nanometer- and micrometer-sized particles. For particles of size comparable to or smaller than the boundary layers, the thermoviscous theory leads to profound consequences for the acoustic radiation force. Not only do we predict forces orders of magnitude larger than expected from ideal-fluid theory, but for certain relevant choices of materials, we also find a sign change in the acoustic radiation force on different-sized but otherwise identical particles. These findings lead to the concept of a particle-size-dependent acoustophoretic contrast factor, highly relevant to acoustic separation of microparticles in gases, as well as to handling of nanoparticles in lab-on-a-chip systems.

DOI: 10.1103/PhysRevE.92.043010 PACS number(s): 47.35.Rs, 43.25.Qp, 43.20.Fn, 43.20.+g

I. INTRODUCTION

The acoustic radiation force is the time-averaged force exerted on a particle in an acoustical field due to scattering of the acoustic waves from the particle. Theoretical studies of the acoustic radiation force date back to King in 1934 [1] and Yosioka and Kawasima in 1955 [2], who considered the force on an incompressible and a compressible particle, respectively, in an inviscid ideal fluid. Their work was summarized and generalized in 1962 by Gorkov [3], with the analysis, however, still limited to ideal fluids and valid only for particles with a radius a much smaller than the acoustic wavelength λ.

In subsequent work, Doinikov developed general theoretical schemes for calculating acoustic radiation forces including viscous and thermoviscous effects [4–6]. The direct applicability of these studies is hampered by the generality of the developed formalism, and analytical expressions are given only in the special limits of $\delta \ll a \ll \lambda$ and $a \ll \delta \ll \lambda$, where δ is the boundary-layer thickness. Similarly, the work of Danilov and Mironov, including viscous effects, only provides analytical expressions in these two limits [7]. However, micrometer-sized particles in water at MHz frequency used in lab-on-a-chip systems for trapping [8–10] and separation [11–21], or in gases at kHz frequency used for separation [22–24] and levitation [25–28], often fall outside of these limits as $\delta \sim a \ll \lambda$. For example, in water at 2 MHz the viscous and thermal boundary layers are of thickness $\delta_s = 0.4\ \mu$m and $\delta_t = 0.2\ \mu$m, respectively, while in air at 50 kHz one finds $\delta_s = 10\ \mu$m and $\delta_t = 12\ \mu$m. Consequently, the acoustic radiation force on nanometer- and micrometer-sized particles is not well described by the limited expressions for small and large boundary layers. The more general case of arbitrary viscous boundary-layer thicknesses compared to the particle size was subsequently studied analytically by Settnes and Bruus in the adiabatic limit where thermal boundary layers are neglected [29]. Their asymptotic study demonstrated that small changes in the scattered field may significantly affect the acoustic radiation force exerted on the particle. Since a thermal boundary layer may also lead to such changes for physically relevant parameters, an extension of the theory in Ref. [29] to include nonadiabatic effects from heat conduction is desirable. Moreover, it is also of interest to extend the treatment of compressible solid particles in Ref. [29] to include droplets or elastic particles for which viscous or elastic shear must be taken into account.

In this work we extend the radiation force theory for droplets and elastic particles to include the effect of both viscosity and heat conduction, thus accounting for the viscous and thermal boundary layers of thicknesses δ_s and δ_t, respectively, and we give closed-form analytical expressions in the limit of $\delta_s, \delta_t, a \ll \lambda$ with no further restrictions between δ_s, δ_t, and a. Our approach to the full thermoviscous scattering problem follows that of Epstein and Carhart from 1953 [30]. The scope of their work was a theory for the absorption of sound in emulsions such as water fog in air. In 1972, Allegra and Hawley further developed the theory to include elastic solid particles suspended in a fluid in order to calculate the attenuation of sound in suspensions and emulsions [31]. The seminal work of those authors has become known as ECAH theory within the field of ultrasound characterization of emulsions and suspensions, and combined with the multiple wave scattering theories of Refs. [32,33] it has been applied to calculate homogenized complex wave numbers of suspensions and emulsions [34,35].

The field of ultrasound characterization driven by engineering applications and the field of acoustic radiation forces have developed in parallel with little overlap. Indeed, the scopes of the work in the two fields are very different. In the works of Epstein and Carhart and Allegra and Hawley, there is no mention of acoustic radiation forces [30,31]. However, the underlying scattering problem of a particle suspended in a fluid remains the same, and having once solved for the amplitude of the propagating scattered wave, the acoustic radiation force on the particle may be obtained from a far-field calculation.

*jonkar@fysik.dtu.dk
†bruus@fysik.dtu.dk

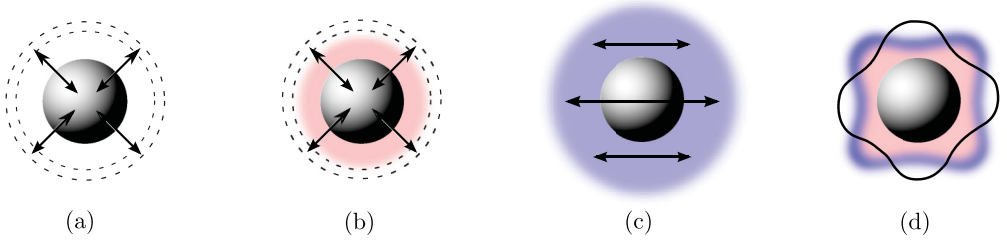

FIG. 1. (Color online) Sketches of the physical mechanisms responsible for various multipole components in the scattering of an incident acoustic wave on a particle. (a) Compressibility contrast: the incident periodic pressure field compresses the particle relative to the fluid, which leads to monopole radiation. (b) Thermal contrast: the incident periodic temperature field leads to thermal expansion of the particle relative to the fluid, which also gives rise to monopole radiation and the development of a diffusive thermal boundary layer (pink). (c) Density contrast: a difference in inertia between particle and fluid causes the particle to oscillate relative to the fluid, which gives rise to dipole radiation and the development of a viscous boundary layer (blue). (d) Particle resonances: acoustic wavelengths comparable to the particle size lead to complex shape changes, which give rise to multipole radiation and a complex thermoviscous boundary layer (pink and blue).

In the far field, the propagating scattered field changes when taking into account the thermoviscous scattering mechanisms, including boundary-layer losses and excitation of acoustic streaming in the vicinity of the particle. In this work we will elucidate this approach, as it leads to a particularly simple and valuable formulation for the acoustic radiation force in the long-wavelength limit [29].

Considering the success of the ECAH method to describe attenuation of sound in emulsions and suspensions, we can with great confidence apply the method to analyze the consequences of thermoviscous scattering on the acoustic radiation force. Nevertheless, we find a need to re-examine the problem of thermoviscous scattering in order to apply the theory to the problem of acoustic radiation forces in a clear and consistent manner. One point of clarification relates to an ambiguity in the thermoelastic solid theory presented by Allegra and Hawley [31], where no clear distinction is made between isothermal and adiabatic solid parameters, thus tacitly implying $\gamma = c_p/c_V = 1$ in solids. Here, we will provide a self-consistent treatment of thermoviscous scattering that clarifies this issue and allows easy comparison with existing acoustic radiation force theories.

Before proceeding with the mathematical treatment, we refer the reader to Fig. 1, which illustrates the physical mechanisms responsible for the monopole, dipole, and multipole scattering from a particle subject to a periodic acoustic field [35]. The final results for the acoustic radiation force are presented in terms of corrected expressions for the monopole and dipole scattering coefficients f_0 and f_1. This approach allows an easy comparison with ideal-fluid theory; moreover, as shown by Settnes and Bruus [29], it provides a simple way of evaluating acoustic radiation forces for any given incident acoustic field. To this end, Table I provides an overview of the equations needed to evaluate the thermoviscous acoustic radiation force on small droplets or solid particles.

TABLE I. References to analytical expressions derived in this paper for the monopole and dipole scattering coefficients f_0 and f_1 in the long-wavelength limit $\delta, a \ll \lambda$. For any given incident acoustic field, the acoustic radiation force $\boldsymbol{F}^{\mathrm{rad}}$ is calculated using Eq. (5) with these expressions for f_0 and f_1.

Size of particle and boundary layers	f_0	f_1
Thermoviscous droplet:		
Arbitrary-width boundary layers	Eq. (59)	Eq. (68)
Small-width boundary layers	Eq. (60)	Eq. (69)
Zero-width boundary layers	Eq. (61)	Eq. (72)
Point-particle limit	Eq. (62)	Eq. (73)
Thermoelastic particle:		
Arbitrary-width boundary layers	Eq. (64)	Eq. (70)
Small-width boundary layers	Eq. (66)	Eq. (71)
Zero-width boundary layers	Eq. (67)	Eq. (72)
Point-particle limit	Eq. (65)	Eq. (73)

II. BASIC CONSIDERATIONS ON THE ACOUSTIC RADIATION FORCE

We consider a single particle or droplet suspended in an infinite, quiescent fluid medium with no net body force, but perturbed by a time-harmonic acoustic field with angular frequency ω. The density, velocity, and stress of the perturbed fluid is denoted ρ, $\boldsymbol{v}$, and $\boldsymbol{\sigma}$, respectively. The region $\Omega(t)$ occupied by the particle, its surface $\partial\Omega(t)$, and the outward-pointing surface vector $\boldsymbol{n}$ depend on time due to the acoustic field. The instantaneous acoustic radiation force is given by the surface integral of the fluid stress $\boldsymbol{\sigma}$ acting on the particle surface. However, since the short time scale corresponding to the oscillation period τ is not resolved experimentally, we define the acoustic radiation force $\boldsymbol{F}^{\mathrm{rad}}$ in the conventional time-averaged sense [1–4,7,29],

$$\boldsymbol{F}^{\mathrm{rad}} = \left\langle \oint_{\partial\Omega(t)} \boldsymbol{\sigma}\cdot\boldsymbol{n}\, da \right\rangle, \tag{1}$$

where the angled bracket denotes the time average over one oscillation period. Notice that this definition includes the acoustic streaming generated locally near the particle, since the stresses leading to this streaming are contained in the fluid stress tensor $\boldsymbol{\sigma}$. In contrast, by considering an infinite domain, we are excluding effects of what Danilov and Mironov refer to as external streaming [7], which would be generated at the boundaries of any finite domain. For a given finite domain, the external streaming can be calculated [36], and the total force acting on a particle is the sum of the radiation force and the external-streaming-induced Stokes drag. This approach

has been used in studies of particle trajectories and has been validated experimentally [37,38].

We consider a state, which is periodic in the acoustic oscillation period τ, tantamount to requiring that any nonperiodic phenomenon, such as particle drift, is negligible within one oscillation period. Usually, this requirement is not very restrictive, as discussed in more detail in Sec. VII. For a time-periodic state, any field can be written as a Fourier series $f(\boldsymbol{r},t) = \sum_{n=0}^{\infty} f_n(\boldsymbol{r})\, e^{-\mathrm{i}n\omega t}$, with $\omega = 2\pi/\tau$, and the time average of any total time derivative is zero, $\langle \frac{d}{dt} f(\boldsymbol{r},t)\rangle = 0$.

A useful expression for $\boldsymbol{F}^{\mathrm{rad}}$ is obtained by considering the momentum flux density $\boldsymbol{\sigma} - \rho\boldsymbol{v}\boldsymbol{v}$ entering the fluid volume between the particle surface $\partial\Omega(t)$ and an arbitrary static surface $\partial\Omega_1$ enclosing the particle. The total momentum $\boldsymbol{P}$ of the fluid in this volume is the volume integral of $\rho\boldsymbol{v}$, and because the net body force on the fluid is zero, the time-averaged rate of change $\langle \frac{d}{dt}\boldsymbol{P}\rangle$ is

$$\left\langle \frac{d\boldsymbol{P}}{dt}\right\rangle = \left\langle \oint_{\partial\Omega_1} [\boldsymbol{\sigma} - \rho\boldsymbol{v}\boldsymbol{v}]\cdot\boldsymbol{n}\, da\right\rangle + \left\langle \oint_{\partial\Omega(t)} \boldsymbol{\sigma}\cdot(-\boldsymbol{n})\, da\right\rangle = \left\langle \oint_{\partial\Omega_1} [\boldsymbol{\sigma} - \rho\boldsymbol{v}\boldsymbol{v}]\cdot\boldsymbol{n}\, da\right\rangle - \boldsymbol{F}^{\mathrm{rad}}. \tag{2}$$

Here, $\boldsymbol{n}$ is the surface vector pointing out of $\partial\Omega_1$ (out of the fluid) and out of $\partial\Omega(t)$ (into the fluid). The advection term $\rho\boldsymbol{v}\boldsymbol{v}$ is zero at $\partial\Omega(t)$, since there is no advection of momentum through the interface of the particle. Finally, using that the time average of the total time derivative $\langle \frac{d\boldsymbol{P}}{dt}\rangle$ is zero in the time-periodic system, we obtain

$$\boldsymbol{F}^{\mathrm{rad}} = \left\langle \oint_{\partial\Omega_1} [\boldsymbol{\sigma} - \rho\boldsymbol{v}\boldsymbol{v}]\cdot\boldsymbol{n}\, da\right\rangle. \tag{3}$$

Thus, even before applying perturbation theory, the acoustic radiation force can be evaluated as the total momentum flux through any static surface $\partial\Omega_1$ enclosing the particle. To second order in the acoustic perturbation, using the expansions $\rho = \rho_0 + \rho_1 + \rho_2$, $\boldsymbol{v} = \boldsymbol{0} + \boldsymbol{v}_1 + \boldsymbol{v}_2$, and $\boldsymbol{\sigma} = \boldsymbol{\sigma}_0 + \boldsymbol{\sigma}_1 + \boldsymbol{\sigma}_2$, the radiation force (3) becomes

$$\boldsymbol{F}^{\mathrm{rad}} = \oint_{\partial\Omega_1} [\langle\boldsymbol{\sigma}_2\rangle - \rho_0\langle\boldsymbol{v}_1\boldsymbol{v}_1\rangle]\cdot\boldsymbol{n}\, da, \tag{4}$$

where we have used that the time average of the time-harmonic, first-order fields is zero.

In regions sufficiently far from acoustic boundary layers, the acoustic wave is a weakly damped propagating acoustic mode, for which viscous and thermal effects are negligible. Thus the result of Ref. [29], obtained by analytically integrating Eq. (4) by placing $\partial\Omega_1$ in the far field, remains valid in the thermoviscous case. In the long-wavelength limit, where the particle radius a is assumed much smaller than the wavelength λ, i.e., for $k_0 a \ll 1$ with $k_0 = 2\pi/\lambda$, it was shown that the acoustic radiation force may be evaluated directly from the incident first-order acoustic field and the expressions for the monopole and dipole scattering coefficients f_0 and f_1 for the suspended particle, as [29]

$$\boldsymbol{F}^{\mathrm{rad}} = -\pi a^3\left[\frac{2\kappa_s}{3}\,\mathrm{Re}[f_0^*\, p_{\mathrm{in}}^*\nabla p_{\mathrm{in}}] - \rho_0\mathrm{Re}[f_1^*\boldsymbol{v}_{\mathrm{in}}^*\cdot\nabla\boldsymbol{v}_{\mathrm{in}}]\right]. \tag{5}$$

Here, p_{in} and $\boldsymbol{v}_{\mathrm{in}}$ are the incident acoustic pressure and velocity fields evaluated at the particle position, the asterisk denotes complex conjugation, and κ_s and ρ_0 are the isentropic compressibility and the mass density of the fluid medium, respectively.

Equation (5) is valid for any incident time-harmonic acoustic field, and consequently the problem of calculating the radiation force on a small particle reduces to calculating the coefficients f_0 and f_1. Closed analytical expressions for these are given in the literature for small particles in the special cases of compressible particles in ideal fluids [2,3] and compressible particles in viscous fluids [29]. Moreover, f_0 and f_1 can be extracted from Refs. [5,6] for rigid spheres and liquid droplets in thermoviscous fluids for the limiting cases of very thin and very thick boundary layers. The main result of this paper is the derivation of analytical expressions for f_0 and f_1 for a spherical thermoviscous droplet and a thermoelastic particle suspended in a thermoviscous fluid without restrictions on the boundary-layer thicknesses, see Table I. Moreover, we provide an analysis of how $\boldsymbol{F}^{\mathrm{rad}}$ is affected by thermoviscous effects in these cases.

Finally, we note that since f_0 and f_1 depend only on frequency and material parameters, expression (5) for the radiation force remains valid for any incident wave composed of plane waves at the same frequency. In the case of a superposition $p_{\mathrm{in}}(\boldsymbol{r},t) = \sum_{n=1}^{N} p_n(\boldsymbol{r})e^{-i\omega_n t}$ of acoustic fields $p_n(\boldsymbol{r})$ (and similarly for $\boldsymbol{v}_{\mathrm{in}}$) at different frequencies ω_n, the resulting radiation force is obtained by summing over the forces obtained from Eq. (5) for each frequency,

$$\boldsymbol{F}^{\mathrm{rad}} = -\pi a^3\sum_{n=1}^{N}\left[\frac{2\kappa_s}{3}\,\mathrm{Re}[f_{0,n}^*\, p_n^*\nabla p_n] - \rho_0\,\mathrm{Re}[f_{1,n}^*\,\boldsymbol{v}_n^*\cdot\nabla\boldsymbol{v}_n]\right]. \tag{6}$$

This generalization of Eq. (5) provides a way to evaluate the acoustic radiation force on a single particle regardless of the complexity of the incident field.

III. THERMOVISCOUS PERTURBATION THEORY OF ACOUSTICS IN FLUIDS

The starting point of the theory is the first law of thermodynamics and the conservation of mass, momentum, and energy. Introducing the thermodynamic variables temperature T, pressure p, density ρ, internal energy ε per mass unit, entropy s per mass unit, and volume per mass unit $1/\rho$, the first law of thermodynamics with s and ρ as independent variables becomes

$$d\varepsilon = T\, ds - p\, d\left(\frac{1}{\rho}\right) = T\, ds + \frac{p}{\rho^2}\, d\rho. \tag{7}$$

For acoustic wave propagation it is often convenient to use T and p as independent thermodynamic variables. This is obtained by a Legendre transformation of the internal energy ε per unit mass to the Gibbs free energy g per unit mass, $g = \varepsilon - Ts + p\,\frac{1}{\rho}$.

Besides the first law of thermodynamics, the governing equations of thermoviscous acoustics require the introduction

of the velocity field $\boldsymbol{v}$ and the stress tensor $\boldsymbol{\sigma}$ of the fluid. The latter can be expressed in terms of $\boldsymbol{v}$, p, the dynamic shear viscosity η, the bulk viscosity η^{b}, and the viscosity ratio $\beta = \eta^{\mathrm{b}}/\eta + 1/3$, as

$$\boldsymbol{\sigma} = -p\,\mathbf{I} + \boldsymbol{\tau}, \tag{8a}$$

$$\boldsymbol{\tau} = \eta[\nabla\boldsymbol{v} + (\nabla\boldsymbol{v})^{\mathrm{T}}] + (\beta - 1)\eta(\nabla\cdot\boldsymbol{v})\,\mathbf{I}. \tag{8b}$$

Here, $\mathbf{I}$ is the unit tensor and the superscript "T" indicates tensor transposition. The tensor $\boldsymbol{\tau}$ is the viscous part of the stress tensor assuming a Newtonian fluid [39].

Considering the fluxes of mass, momentum, and energy into a small test volume, we use Gauss's theorem to formulate the general governing equations for conservation of mass, momentum, and energy in the fluid under the assumption of no net body forces and no heat sources,

$$\partial_t\rho = \nabla\cdot[-\rho\boldsymbol{v}], \tag{9a}$$

$$\partial_t(\rho\boldsymbol{v}) = \nabla\cdot[\boldsymbol{\sigma} - \rho\boldsymbol{v}\boldsymbol{v}], \tag{9b}$$

$$\partial_t\left(\rho\varepsilon + \tfrac{1}{2}\rho v^2\right) = \nabla\cdot\left[\boldsymbol{v}\cdot\boldsymbol{\sigma} + k_{\mathrm{th}}\nabla T - \rho\left(\varepsilon + \tfrac{1}{2}v^2\right)\boldsymbol{v}\right]. \tag{9c}$$

Here, we have introduced the thermal conductivity k_{th} assuming the usual linear form for the heat flux given by Fourier's law of heat conduction.

A. First-order equations for fluids

The zeroth-order state of the fluid is quiescent, homogeneous, and isotropic. Then, treating the acoustic field as a perturbation of this state in the acoustic perturbation parameter $\varepsilon_{\mathrm{ac}}$, given by

$$\varepsilon_{\mathrm{ac}} = \frac{|\rho_1|}{\rho_0} \ll 1, \tag{10}$$

we expand all fields as $g = g_0 + g_1$, but with $\boldsymbol{v}_0 = \mathbf{0}$. The zeroth-order terms drop out of the governing equations, while the first-order mass, momentum, and energy equations obtained from Eqs. (7) and (9) become

$$\partial_t\rho_1 = -\rho_0\nabla\cdot\boldsymbol{v}_1, \tag{11a}$$

$$\rho_0\partial_t\boldsymbol{v}_1 = -\nabla p_1 + \eta_0\nabla^2\boldsymbol{v}_1 + \beta\eta_0\nabla(\nabla\cdot\boldsymbol{v}_1), \tag{11b}$$

$$\rho_0 T_0\partial_t s_1 = k_{\mathrm{th}}\nabla^2 T_1. \tag{11c}$$

It will prove useful to eliminate the variables p_1, ρ_1, and s_1 to end up with only two equations for the variables $\boldsymbol{v}_1$ and T_1. To this end, we combine Eq. (11) with the two thermodynamic equations of state $\rho = \rho(p, T)$ and $s = s(p, T)$. The total differentials of ρ and s are

$$d\rho = \left(\frac{\partial\rho}{\partial p}\right)_T dp + \left(\frac{\partial\rho}{\partial T}\right)_p dT, \tag{12a}$$

$$ds = \left(\frac{\partial s}{\partial p}\right)_T dp + \left(\frac{\partial s}{\partial T}\right)_p dT, \tag{12b}$$

which may be linearized so that the partial derivatives of ρ and s refer to the unperturbed state of the fluid. This leads to the introduction of the isothermal compressibility κ_T, the isobaric thermal expansion coefficient α_p, and the specific heat capacity at constant pressure c_p,

$$\kappa_T = \frac{1}{\rho}\left(\frac{\partial\rho}{\partial p}\right)_T, \quad \alpha_p = -\frac{1}{\rho}\left(\frac{\partial\rho}{\partial T}\right)_p,$$
$$c_p = T\left(\frac{\partial s}{\partial T}\right)_p. \tag{13}$$

Moreover, $(\partial s/\partial p)_T = -\alpha_p/\rho$, which may be derived as a Maxwell relation differentiating g after p and T. Thus, the linearized form of Eq. (12) is

$$\rho_1 = \rho_0\,\kappa_T\,p_1 - \rho_0\,\alpha_p\,T_1, \tag{14a}$$

$$s_1 = \frac{c_p}{T_0}\,T_1 - \frac{\alpha_p}{\rho_0}\,p_1. \tag{14b}$$

We further introduce the isentropic compressibility κ_s and the specific heat capacity at constant volume c_V,

$$\kappa_s = \frac{1}{\rho}\left(\frac{\partial\rho}{\partial p}\right)_s, \quad c_V = T\left(\frac{\partial s}{\partial T}\right)_V. \tag{15}$$

Then the following two well-known thermodynamic identities may be derived [40]:

$$\kappa_T = \gamma\kappa_s, \quad \gamma \equiv \frac{c_p}{c_V} = 1 + \frac{\alpha_p^2 T_0}{\rho_0 c_p\kappa_s}. \tag{16}$$

To proceed with the reduction of Eq. (11), we first differentiate Eq. (11b) with respect to time and substitute $\nabla^2\boldsymbol{v}_1 = \nabla(\nabla\cdot\boldsymbol{v}_1) - \nabla\times\nabla\times\boldsymbol{v}_1$. Then, Eq. (14) is used to eliminate p_1 and s_1 in Eqs. (11b) and (11c), followed by elimination of $\partial_t\rho_1$ using Eq. (11a). The resulting equations for $\boldsymbol{v}_1$ and T_1 are

$$\partial_t^2\boldsymbol{v}_1 - \left(\frac{1}{\rho_0\kappa_T} + (1+\beta)\nu_0\partial_t\right)\nabla(\nabla\cdot\boldsymbol{v}_1) + \nu_0\partial_t\nabla\times\nabla\times\boldsymbol{v}_1 = -\frac{\alpha_p}{\rho_0\kappa_T}\partial_t\nabla T_1, \tag{17a}$$

$$\gamma D_{\mathrm{th}}\nabla^2 T_1 - \partial_t T_1 = \frac{\gamma - 1}{\alpha_p}\nabla\cdot\boldsymbol{v}_1, \tag{17b}$$

where we have introduced the momentum diffusion constant ν_0 and the thermal diffusion constant D_{th},

$$\nu_0 = \frac{\eta_0}{\rho_0}, \quad D_{\mathrm{th}} = \frac{k_{\mathrm{th}}}{\rho_0 c_p}. \tag{18}$$

B. Potential equations for fluids

The velocity field $\boldsymbol{v}_1$ is decomposed into the gradient of a scalar potential ϕ (the longitudinal component) and the rotation of a divergence-free vector potential $\boldsymbol{\psi}$ (the transverse component),

$$\boldsymbol{v}_1 = \nabla\phi + \nabla\times\boldsymbol{\psi}, \ \text{with}\ \nabla\cdot\boldsymbol{\psi} = 0. \tag{19}$$

Inserting this well-known Helmholtz decomposition into Eq. (17a) leads to the equation

$$\nabla\left[\partial_t^2\phi - \left(\frac{1}{\rho_0\kappa_T} + (1+\beta)\nu_0\partial_t\right)\nabla^2\phi + \frac{\alpha_p}{\rho_0\kappa_T}\partial_t T_1\right] = \nabla\times\left[-\partial_t^2\boldsymbol{\psi} + \nu_0\partial_t\nabla^2\boldsymbol{\psi}\right]. \tag{20}$$

In general, both sides of the equation must vanish separately, which leads to two equations. Combining these with Eq. (17b), into which Eq. (19) is inserted, leads to the following form of Eq. (17):

$$\partial_t^2\phi = \left(\frac{1}{\rho_0\kappa_T} + (1+\beta)\nu_0\partial_t\right)\nabla^2\phi - \frac{\alpha_p}{\rho_0\kappa_T}\partial_t T_1, \quad (21a)$$

$$\partial_t T_1 = \gamma D_{\rm th}\nabla^2 T_1 - \frac{\gamma-1}{\alpha_p}\nabla^2\phi, \quad (21b)$$

$$\partial_t \boldsymbol{\psi} = \nu_0\nabla^2\boldsymbol{\psi}. \quad (21c)$$

In the adiabatic limit, for which $D_{\rm th} = 0$, the well-known adiabatic wave equation for ϕ is obtained by inserting Eq. (21b) into (21a), from which the adiabatic speed of sound c for longitudinal waves is deduced,

$$c = \frac{1}{\sqrt{\rho_0\kappa_s}}. \quad (22)$$

In the isothermal case, for which $T_1 = 0$, the wave equation (21a) instead describes waves traveling at the isothermal speed of sound $c/\sqrt{\gamma} = 1/\sqrt{\rho_0\kappa_T}$. For ultrasound acoustics, sound propagation in the bulk of a fluid is generally very close to being adiabatic.

IV. THERMOELASTIC THEORY OF ACOUSTICS IN ISOTROPIC SOLIDS

A thermoelastic solid may be deformed by the action of applied forces or on account of thermal expansion. Following Landau and Lifshitz [41], we describe the deformation of a solid elastic body using the displacement field $\boldsymbol{u}$, which describes the displacement $\boldsymbol{u}(\boldsymbol{r},t)$ of a solid element away from its initial, undeformed position $\boldsymbol{r}$ to its new temporary position $\boldsymbol{r} + \boldsymbol{u}(\boldsymbol{r},t)$. Any displacement away from equilibrium gives rise to internal stresses tending to return the body to equilibrium. These forces are described using the stress tensor $\boldsymbol{\sigma}$, which leads to the force density $\boldsymbol{\nabla}\cdot\boldsymbol{\sigma}$. In the description of the thermodynamics of solids, it is advantageous to work with per-volume quantities denoted by uppercase letters, in contrast to the per-mass quantities given by lowercase letters. The first law of thermodynamics reads

$$d\mathcal{E} = TdS + \sigma_{ij}du_{ij}, \quad (23)$$

where $\mathcal{E}$ is the internal energy per unit volume, S is the entropy per unit volume, and T is the temperature. The work done by the internal stresses per unit volume is equal to $-\sigma_{ij}du_{ij}$, where we have introduced the strain tensor u_{ij}, which for small displacements is given by

$$u_{ij} = \tfrac{1}{2}[\partial_i u_j + \partial_j u_i]. \quad (24)$$

Transforming the internal energy per unit volume $\mathcal{E}$ to the Helmholtz free energy per unit volume $F = \mathcal{E} - TS$, where temperature T and strain u_{ij} are the independent variables, the first law becomes $dF = -SdT + \sigma_{ij}du_{ij}$.

Consider the undeformed state of an isotropic, thermoelastic solid at temperature T_0 in the absence of external forces. The free energy F is then given as an expansion in powers of the temperature difference $T - T_0$ and the strain tensor u_{ij}. To linear order, the stress tensor $\sigma_{ij} = (\frac{\partial F}{\partial u_{ij}})_T$ and the entropy $S = -(\frac{\partial F}{\partial T})_{u_{ij}}$ become

$$\sigma_{ij} = -\frac{\alpha_p(T-T_0)}{\kappa_T}\delta_{ij} + \frac{E}{1+\sigma}\left[u_{ij} + \frac{\sigma}{1-2\sigma}u_{kk}\delta_{ij}\right], \quad (25a)$$

$$S(T) = S_0(T) + \frac{\alpha_p}{\kappa_T}u_{kk}, \quad (25b)$$

where $S_0(T)$ is the entropy of the undeformed state at temperature T, while E and σ are the isothermal Young's modulus and Poisson's ratio, respectively. The isothermal compressibility κ_T of the solid is given in terms of E and σ as

$$\kappa_T = 3(1-2\sigma)\frac{1}{E}. \quad (26)$$

A. Linear equations for solids

In elastic solids, advection of momentum and heat cannot occur, so the momentum equation in the absence of body forces takes the linear form $\rho\partial_t^2\boldsymbol{u} = \boldsymbol{\nabla}\cdot\boldsymbol{\sigma}$. Assuming the material parameters α_p, κ_T, E, and σ to be constant, it becomes

$$\begin{aligned}\rho\partial_t^2\boldsymbol{u} &= -\frac{\alpha_p}{\kappa_T}\boldsymbol{\nabla}T + \frac{E}{2(1+\sigma)}\left[\nabla^2\boldsymbol{u} + \frac{1}{1-2\sigma}\boldsymbol{\nabla}(\boldsymbol{\nabla}\cdot\boldsymbol{u})\right]\\ &= -\frac{\alpha_p}{\rho\kappa_T}\boldsymbol{\nabla}T + c_{\rm T}^2\nabla^2\boldsymbol{u} + \left(c_{\rm L}^2 - c_{\rm T}^2\right)\boldsymbol{\nabla}(\boldsymbol{\nabla}\cdot\boldsymbol{u}), \quad (27)\end{aligned}$$

where we have introduced the isothermal speed of sound of longitudinal waves $c_{\rm L}$ and of transverse waves $c_{\rm T}$,

$$c_{\rm L}^2 = \frac{(1-\sigma)}{(1+\sigma)(1-2\sigma)}\frac{E}{\rho}, \quad c_{\rm T}^2 = \frac{1}{2(1+\sigma)}\frac{E}{\rho}. \quad (28a)$$

Using the decomposition $\boldsymbol{u} = \boldsymbol{u}_{\rm T} + \boldsymbol{u}_{\rm L}$ in the transverse and longitudinal displacements $\boldsymbol{u}_{\rm T}$ and $\boldsymbol{u}_{\rm L}$ with $\boldsymbol{\nabla}\cdot\boldsymbol{u}_{\rm T} = 0$ and $\boldsymbol{\nabla}\times\boldsymbol{u}_{\rm L} = \boldsymbol{0}$, respectively, it immediately follows from Eq. (27) that in the isothermal case, transverse and longitudinal waves travel at the speed $c_{\rm T}$ and $c_{\rm L}$, respectively. Combining Eqs. (26) and (28a) one obtains an important relation connecting the isothermal compressibility κ_T of the solid to the isothermal sound speeds $c_{\rm L}$ and $c_{\rm T}$,

$$\frac{1}{\rho\kappa_T} = c_{\rm L}^2 - \frac{4}{3}c_{\rm T}^2. \quad (28b)$$

Turning to the energy equation, the amount of heat absorbed per unit time per unit volume is $T(\partial_t S)$. If there are no heat sources in the bulk, the rate of heat absorbed is given by the influx $-k_{\rm th}\boldsymbol{\nabla}T$ of heat by conduction, and the heat equation thus becomes

$$T(\partial_t S) = -\boldsymbol{\nabla}\cdot[-k_{\rm th}\boldsymbol{\nabla}T] = k_{\rm th}\nabla^2 T, \quad (29)$$

where the heat conductivity $k_{\rm th}$ is taken to be constant. We rewrite this equation using expression (25b) for the entropy, and using that the time derivative of S_0 may be written as

$$\frac{\partial S_0}{\partial t} = \left(\frac{\partial S_0}{\partial T}\right)_V\frac{\partial T}{\partial t} = \frac{C_V}{T}\frac{\partial T}{\partial t}, \quad (30)$$

where the heat capacity C_V per unit volume at constant volume enters through the relation $C_V = T\,(\partial S_0/\partial T)_V$ with the

derivative taken for the undeformed state at constant volume, that is, for $u_{kk} = \nabla \cdot \boldsymbol{u} = 0$. Combining these considerations with the identity for γ equivalent to Eq. (16), the heat equation (29) becomes

$$C_V \partial_t T + \frac{(\gamma - 1)C_V}{\alpha_p} \partial_t \nabla \cdot \boldsymbol{u} = k_{\mathrm{th}} \nabla^2 T. \tag{31}$$

Finally, having eliminated all extensive thermodynamic variables, we return to per-mass quantities, such as $c_V = C_V/\rho$, and thus arrive at the coupled equations for thermoelastic solids,

$$\partial_t^2 \boldsymbol{u}_1 - c_{\mathrm{L}}^2 \nabla(\nabla \cdot \boldsymbol{u}_1) + c_{\mathrm{T}}^2 \nabla \times \nabla \times \boldsymbol{u}_1 = -\frac{\alpha_p}{\rho_0 \kappa_T} \nabla T_1, \tag{32a}$$

$$\gamma D_{\mathrm{th}} \nabla^2 T_1 - \partial_t T_1 = \frac{\gamma - 1}{\alpha_p} \partial_t \nabla \cdot \boldsymbol{u}_1, \tag{32b}$$

with γ and D_{th} defined in Eqs. (16) and (18), and the linearity emphasized by the addition of subscripts "1" to the field variables. In this form, the thermoelastic equations (32) correspond to the fluid equations (17).

B. Potential equations for solids

The time derivative $\partial_t \boldsymbol{u}_1$ of the displacement field $\boldsymbol{u}_1$ describes the velocity field in the solid. Analogous to the fluid case, we make a Helmholtz decomposition of this velocity field in terms of the velocity potentials ϕ and $\boldsymbol{\psi}$

$$\partial_t \boldsymbol{u}_1 = \nabla \phi + \nabla \times \boldsymbol{\psi}, \text{ with } \nabla \cdot \boldsymbol{\psi} = 0. \tag{33}$$

Inserting this into Eq. (32) and following the procedure leading to Eq. (21) for fluids, we obtain the corresponding three equations for solids:

$$\partial_t^2 \phi = c_{\mathrm{L}}^2 \nabla^2 \phi - \frac{\alpha_p}{\rho_0 \kappa_T} \partial_t T_1, \tag{34a}$$

$$\partial_t T_1 = \gamma D_{\mathrm{th}} \nabla^2 T_1 - \frac{\gamma - 1}{\alpha_p} \nabla^2 \phi, \tag{34b}$$

$$\partial_t^2 \boldsymbol{\psi} = c_{\mathrm{T}}^2 \nabla^2 \boldsymbol{\psi}. \tag{34c}$$

The main difference between the fluid and the solid case is in Eq. (34c) for the vector potential $\boldsymbol{\psi}$, which now takes the form of a wave equation describing transverse waves traveling at the transverse speed of sound c_{T} instead of the diffusion equation (21c).

The usual adiabatic wave equation for the scalar potential ϕ is obtained in the limit of $D_{\mathrm{th}} = 0$ combining Eqs. (34a) and (34b), and the speed c of adiabatic, longitudinal wave propagation in an elastic solid becomes

$$c^2 = c_{\mathrm{L}}^2 + \frac{\gamma - 1}{\rho_0 \kappa_T}. \tag{35}$$

For most solids, $\gamma - 1 \ll 1$, leading to a negligible difference between the isothermal c_{L} and the adiabatic c, the latter being closest to the actual speed of sound measured in ultrasonic experiments.

V. UNIFIED POTENTIAL THEORY OF ACOUSTICS IN FLUIDS AND SOLIDS

The similarity between the potential equations (21) and (34) allows us to write down a unified potential theory of acoustics in thermoviscous fluids and thermoelastic solids. The main result of this section is the derivation of three wave equations with three distinct wave numbers corresponding to three modes of wave propagation, namely, two longitudinal modes describing propagating compressional waves and damped thermal waves and one transverse mode describing a shear wave, which is damped in a fluid but propagating in a solid.

We work with the first-order fields in the frequency domain considering a single frequency ω. Using complex notation, we write any first-order field $g_1(\boldsymbol{r},t)$ as

$$g_1(\boldsymbol{r},t) = g_1(\boldsymbol{r})\, e^{-i\omega t}. \tag{36}$$

Assuming this form of time-harmonic first-order field, Eqs. (21a) and (34a) lead to expressions for the temperature field T_1 in a fluid (fl) and a solid (sl), respectively, in terms of the corresponding scalar potential ϕ

$$T_1^{\mathrm{fl}} = \frac{i\omega\rho_0\kappa_T}{\alpha_p}\left[\phi + \frac{c^2}{\omega^2}\frac{1 - i\gamma\Gamma_{\mathrm{s}}}{\gamma}\nabla^2\phi\right], \tag{37a}$$

$$T_1^{\mathrm{sl}} = \frac{i\omega\rho_0\kappa_T}{\alpha_p}\left[\phi + \frac{c_{\mathrm{L}}^2}{\omega^2}\nabla^2\phi\right]. \tag{37b}$$

Here, we have introduced the dimensionless bulk damping factor Γ_{s} accounting for viscous dissipation in the fluid. For convenience, we also introduce the thermal damping factor Γ_{t} accounting for dissipation due to heat conduction both in fluids and in solids. These two bulk damping factors are given by

$$\Gamma_{\mathrm{s}} = \frac{(1 + \beta)\nu_0\omega}{c^2}, \quad \Gamma_{\mathrm{t}} = \frac{D_{\mathrm{th}}\omega}{c^2}. \tag{38}$$

Substituting expression (37a) for T_1^{fl} into Eq. (21b), or expression (37b) for T_1^{sl} into Eq. (34b), and assuming time-harmonic fields [Eq. (36)], we eliminate the temperature field and obtain a biharmonic equation for the scalar potential ϕ,

$$\alpha_{\mathrm{xl}}\nabla^2\nabla^2\phi + \beta_{\mathrm{xl}}k_0^2\nabla^2\phi + k_0^4\phi = 0, \quad \text{with} \quad k_0 = \frac{\omega}{c}, \tag{39a}$$

where we have introduced the undamped adiabatic wave number $k_0 = \omega/c$, and where the parameters α_{xl} and β_{xl} for fluids (xl = fl) and solids (xl = sl) are

$$\alpha_{\mathrm{fl}} = -i(1 - i\gamma\Gamma_{\mathrm{s}})\Gamma_{\mathrm{t}}, \quad \beta_{\mathrm{fl}} = 1 - i(\Gamma_{\mathrm{s}} + \gamma\Gamma_{\mathrm{t}}), \tag{39b}$$

$$\alpha_{\mathrm{sl}} = -i(1 + X)\Gamma_{\mathrm{t}}, \quad \beta_{\mathrm{sl}} = 1 - i\gamma\Gamma_{\mathrm{t}}. \tag{39c}$$

Here, we have used relation (35) for solids and further introduced the parameters X and χ,

$$X = (\gamma - 1)(1 - \chi), \tag{39d}$$

$$\chi = \frac{1}{\rho_0\kappa_s c^2} = 1 - \frac{4}{3}\frac{c_{\mathrm{T}}^2}{c^2}, \tag{39e}$$

the latter equality following from combining Eq. (35) with Eq. (28b) and using $\kappa_T = \gamma\kappa_s$ from Eq. (16). Note that for fluids, $\chi = 1$, $c_{\mathrm{T}} = 0$, and $X = 0$.

The biharmonic equation (39a) is factorized and written on the equivalent form

$$\left(\nabla^2 + k_c^2\right)\left(\nabla^2 + k_t^2\right)\phi = 0, \tag{40a}$$

and thus the wave numbers k_c and k_t are obtained from $k_c^2 + k_t^2 = \beta_{xl} k_0^2/\alpha_{xl}$ and $k_c^2 k_t^2 = k_0^4/\alpha_{xl}$, resulting in

$$k_c^2 = 2k_0^2\left[\beta_{xl} + \left(\beta_{xl}^2 - 4\alpha_{xl}\right)^{1/2}\right]^{-1}, \tag{40b}$$

$$k_t^2 = 2k_0^2\left[\beta_{xl} - \left(\beta_{xl}^2 - 4\alpha_{xl}\right)^{1/2}\right]^{-1}, \tag{40c}$$

with "xl" being either "fl" for fluids or "sl" for solids.

In the frequency domain, the equation for the vector potential $\boldsymbol{\psi}$, Eq. (21c) for fluids and Eq. (34c) for solids, can be written as $\nabla^2\boldsymbol{\psi} + k_s^2\boldsymbol{\psi} = \mathbf{0}$, which describes a transverse shear mode with shear wave number k_s. By introducing a shear constant η_0, which for a fluid is the dynamic viscosity, and for a solid is defined as

$$\eta_0 = i\,\frac{\rho_0 c_T^2}{\omega} \quad \text{(solid)}, \tag{41a}$$

the shear wave number k_s is given by the same expression for both fluids and solids,

$$k_s^2 = \frac{i\omega\rho_0}{\eta_0} \quad \text{(fluid and solid)}. \tag{41b}$$

A. Wave equations and modes

The general solution ϕ of the biharmonic equation (40a) is the sum

$$\phi = \phi_c + \phi_t \tag{42}$$

of the two potentials ϕ_c and ϕ_t, which satisfy the harmonic equations

$$\nabla^2\phi_c + k_c^2\phi_c = 0, \tag{43a}$$

$$\nabla^2\phi_t + k_t^2\phi_t = 0, \tag{43b}$$

where ϕ_c describes a compressional propagating mode with wave number k_c, while ϕ_t describes a thermal mode with wave number k_t. These two scalar wave equations together with the vector wave equation for $\boldsymbol{\psi}$, describing the shear mode with wave number k_s,

$$\nabla^2\boldsymbol{\psi} + k_s^2\boldsymbol{\psi} = \mathbf{0}, \tag{43c}$$

comprise the full set of first-order equations in potential theory. These wave equations, coupled through the boundary conditions, govern acoustics in thermoviscous fluids and thermoelastic solids. The distinction between fluids and solids is to be found solely in the wave numbers of the three modes.

1. Approximate wave numbers for fluids

For most systems of interest, $\Gamma_s, \Gamma_t \ll 1$ allowing a simplification of the expressions for k_c and k_t in Eq. (40). To first order in Γ_s and Γ_t one finds

$$k_c = \frac{\omega}{c}\left[1 + \frac{i}{2}[\Gamma_s + (\gamma - 1)\Gamma_t]\right], \tag{44a}$$

$$k_t = \frac{(1+i)}{\delta_t}\left[1 + \frac{i}{2}(\gamma - 1)(\Gamma_s - \Gamma_t)\right], \tag{44b}$$

$$k_s = \frac{(1+i)}{\delta_s}, \tag{44c}$$

where we have introduced the thermal diffusion length δ_t and the momentum diffusion length δ_s. Heat and momentum diffuses from boundaries, such that the characteristic thicknesses of the thermal and viscous boundary layers are δ_t and δ_s, respectively, given by

$$\delta_t = \sqrt{\frac{2D_{th}}{\omega}}, \quad \delta_s = \sqrt{\frac{2\nu_0}{\omega}}. \tag{45}$$

For water at room temperature and 2 MHz frequency, $\delta_s \simeq 0.4\ \mu$m, $\delta_t \simeq 0.2\ \mu$m, and $\lambda \simeq 760\ \mu$m. Consequently, the length scales of the thermal and viscous boundary-layer thicknesses are the same order of magnitude and much smaller than the acoustic wavelength. With $k_0 = \omega/c$ we note that

$$\Gamma_s = \tfrac{1}{2}(1+\beta)(k_0\delta_s)^2, \quad \Gamma_t = \tfrac{1}{2}(k_0\delta_t)^2, \tag{46}$$

and consequently

$$\Gamma_s \sim (k_0\delta_s)^2 \sim \left|\frac{k_c}{k_s}\right|^2 \ll 1, \tag{47a}$$

$$\Gamma_t \sim (k_0\delta_t)^2 \sim \left|\frac{k_c}{k_t}\right|^2 \ll 1. \tag{47b}$$

In the long-wavelength limit of the scattering theory to be developed, we expand to first order in $k_0\delta_s$ and $k_0\delta_t$, and thus neglect the second-order quantities Γ_s and Γ_t. For water at room temperature and MHz frequency one finds $k_0\delta_s \sim k_0\delta_t \sim 10^{-3}$, and $\Gamma_s \sim \Gamma_t \sim 10^{-6}$.

Clearly, the compressional mode with wave number k_c describes a weakly damped propagating wave with $\mathrm{Im}[k_c] \ll \mathrm{Re}[k_c] \simeq \omega/c$. In contrast, $\mathrm{Im}[k_t] \simeq \mathrm{Re}[k_t]$ for the thermal mode and $\mathrm{Im}[k_s] = \mathrm{Re}[k_s]$ for the shear mode, which correspond to waves that are damped within their respective wavelengths. Hence, these modes describe boundary layers near interfaces of walls and particles, which decay exponentially away from these interfaces on the length scales set by δ_t and δ_s.

2. Approximate wave numbers for solids

Similar to the fluid case, we use the smallness of the thermal damping factor, $\Gamma_t \ll 1$, to expand the exact wave numbers of Eq. (40). To first order we obtain

$$k_c = \frac{\omega}{c}\left[1 + \frac{i}{2}(\gamma - 1)\chi\Gamma_t\right], \tag{48a}$$

$$k_t = \frac{(1+i)}{\delta_t}\frac{1}{\sqrt{1-X}}\left[1 + \frac{i}{8}\frac{\gamma^2\Gamma_t}{(1-X)}\right], \tag{48b}$$

$$k_s = \frac{\omega}{c_T}. \tag{48c}$$

An important distinction between a fluid and a solid is that a solid allows propagating transverse waves while a fluid does not. This is evident from the shear mode wave number k_s, which for solids is purely real, $k_s = \omega/c_T$, while for fluids $\mathrm{Im}[k_s] = \mathrm{Re}[k_s] = 1/\delta_s$.

B. Acoustic fields from potentials

For a given thermoacoustic problem, the boundary conditions are imposed on the acoustic fields $\boldsymbol{v}_1$, T_1, and $\boldsymbol{\sigma}_1$ and not directly on the potentials ϕ_c, ϕ_t, and $\boldsymbol{\psi}$. We therefore need expressions for the acoustic fields in terms of the potentials in order to derive the boundary conditions for the latter.

The velocity fields follow trivially from the Helmholtz decompositions and are obtained from the same expression in both fluids and solids:

$$\boldsymbol{v}_1 = \nabla(\phi_c + \phi_t) + \nabla \times \boldsymbol{\psi}, \quad \text{where} \quad \boldsymbol{v}_1 = -i\omega \boldsymbol{u}_1 \text{ for solids.} \tag{49}$$

A single expression for T_1 in terms of ϕ_c and ϕ_t, valid for both fluids and solids, is obtained from Eq. (37) in combination with Eqs. (40)–(43) by introducing the material-dependent parameters b_c and b_t,

$$T_1 = b_c\phi_c + b_t\phi_t, \tag{50a}$$

$$b_c = \frac{i\omega(\gamma - 1)}{\alpha_p c^2}, \quad b_t = \frac{1}{\chi \alpha_p D_{th}}. \tag{50b}$$

Here, we have neglected Γ_s and Γ_t relative to unity. Note that the ratio $b_c/b_t \sim \Gamma_t \ll 1$.

In a fluid, the pressure field p_1 is obtained by inserting Eq. (19) into the momentum equation (11b) and using the wave equations (43),

$$p_1 = i\omega\rho_0(\phi_c + \phi_t) - (1 + \beta)\eta_0\left(k_c^2\phi_c + k_t^2\phi_t\right). \tag{51}$$

Inserting this expression into Eq. (8a), the stress tensor for fluids becomes

$$\boldsymbol{\sigma}_1 = \eta_0\left[\left(2k_c^2 - k_s^2\right)\phi_c + \left(2k_t^2 - k_s^2\right)\phi_t\right]\mathbf{I} + \eta_0[\nabla \boldsymbol{v}_1 + (\nabla \boldsymbol{v}_1)^T], \tag{52}$$

where $\boldsymbol{v}_1$ can be expressed by the potentials through Eq. (49). This expression also holds true for the solid stress tensor in Eq. (25a) using the shear constant η_0, Eq. (41a), and the velocity field $\boldsymbol{v}_1 = -i\omega\boldsymbol{u}_1$, Eq. (33). This conclusion is obtained by inserting Eq. (37b) for T_1^{sl} into Eq. (25a) for $\boldsymbol{\sigma}_1$ and using the wave equations (43).

VI. SCATTERING FROM A SPHERE

The potential theory allows us in a unified manner to treat linear scattering of an acoustic wave on a spherical particle, consisting of either a thermoelastic solid or a thermoviscous fluid. The system of equations describing the general case of an arbitrary particle size is given, and analytical solutions are provided in the long-wavelength limit $a, \delta_s, \delta_t \ll \lambda$. In this limit, the particle and boundary layers are much smaller than the acoustic wavelength, but the ratios δ_s/a and δ_t/a are unrestricted. This is essential for applying our results to micro- and nanoparticle acoustophoresis. In particular, we derive analytical expressions for the monopole and dipole scattering coefficients f_0 and f_1, which together with the incident acoustic field serve to calculate the acoustic radiation force as shown in Sec. II and summarized in Table I.

A. System setup

We place the spherical particle of radius a at the center of the coordinate system and use spherical coordinates (r,θ,φ) with the radial distance r, the polar angle θ, and the azimuthal angle φ. We let unprimed variables and parameters characterize the region of the fluid medium, $r > a$, while primed variables and parameters characterize the region of the particle, $r < a$. For example, the parameter κ_s' is the compressibility of the particle, while κ_s is the compressibility of the fluid medium. Ratios of particle and fluid parameters are denoted by a tilde, e.g. $\tilde{\kappa}_s = \kappa_s'/\kappa_s$. Due to linearity, we can without loss of generality assume that in the vicinity of the particle, the incident wave is a plane wave propagating in the positive z direction, $\phi_i = \phi_0\, e^{ik_c z} = \phi_0\, e^{ik_c r\cos\theta}$. The fields do not depend on φ due to azimuthal symmetry.

B. Partial wave expansion

The solution to the scalar and the vector wave equations [Eq. (43)] with wave numbers k [Eqs. (44) and (48)] in spherical coordinates is standard textbook material. Avoiding singular solutions at $r = 0$ and considering outgoing scattered waves, the solution is written in terms of spherical Bessel functions $j_n(kr)$, outgoing spherical Hankel functions $h_n(kr)$, and Legendre polynomials $P_n(\cos\theta)$. As a consequence of azimuthal symmetry, only the φ component of the vector potential is nonzero, $\boldsymbol{\psi}(\boldsymbol{r}) = \psi_s(r,\theta)\,\boldsymbol{e}_\varphi$. The solution is written as a partial wave expansion of the incident propagating wave ϕ_i, the scattered reflected propagating wave ϕ_r, the scattered thermal wave ϕ_t, and the scattered shear wave ψ_s:

In the fluid medium, $r > a$

$$\phi_i = \phi_0 \sum_{n=0}^{\infty} i^n(2n+1) j_n(k_c r) P_n(\cos\theta), \tag{53a}$$

$$\phi_r = \phi_0 \sum_{n=0}^{\infty} i^n(2n+1) A_n h_n(k_c r) P_n(\cos\theta), \tag{53b}$$

$$\phi_t = \phi_0 \sum_{n=0}^{\infty} i^n(2n+1) B_n h_n(k_t r) P_n(\cos\theta), \tag{53c}$$

$$\psi_s = \phi_0 \sum_{n=0}^{\infty} i^n(2n+1) C_n h_n(k_s r) \partial_\theta P_n(\cos\theta). \tag{53d}$$

In the particle, $r < a$

$$\phi_c' = \phi_0 \sum_{n=0}^{\infty} i^n(2n+1) A_n' j_n(k_c' r) P_n(\cos\theta), \tag{53e}$$

$$\phi_t' = \phi_0 \sum_{n=0}^{\infty} i^n(2n+1) B_n' j_n(k_t' r) P_n(\cos\theta), \tag{53f}$$

$$\psi_s' = \phi_0 \sum_{n=0}^{\infty} i^n(2n+1) C_n' j_n(k_s' r) \partial_\theta P_n(\cos\theta), \tag{53g}$$

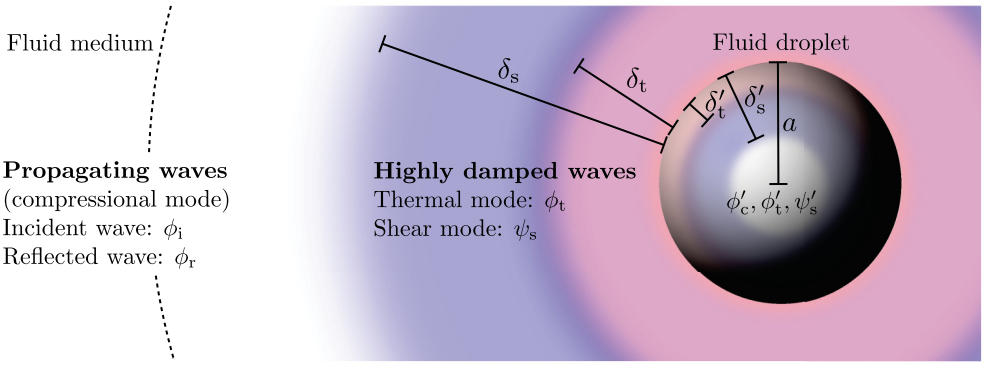

FIG. 2. (Color online) A compressional wave ϕ_i propagating in a thermoviscous fluid medium with parameters $\rho_0,\eta_0,\kappa_s,\alpha_p,c_p,\gamma$, and k_{th}, is incident on a thermoviscous fluid droplet with parameters $\rho'_0,\eta'_0,\kappa'_s,\alpha'_p,c'_p,\gamma'$, and k'_{th}, which results in a compressional scattered wave and highly damped thermal and shear waves both outside in the fluid medium (ϕ_r,ϕ_t,ψ_s) and inside in the fluid droplet $(\phi'_c,\phi'_t,\psi'_s)$. Viscous and thermal boundary layers are described by the highly damped waves both outside and inside the fluid droplet. In the long-wavelength limit the droplet radius a and the boundary-layer thicknesses $\delta_s,\delta_t,\delta'_s,\delta'_t$ are mutually unrestricted, but all much smaller than the acoustic wavelength λ. For a thermoelastic particle, the shear mode ψ'_s describes a propagating transverse wave instead of an internal viscous boundary layer.

where the parameter ϕ_0 is an arbitrary amplitude of the incident wave with unit $m^2\,s^{-1}$. The different components of the resulting acoustic field are illustrated in Fig. 2.

C. Boundary conditions

Neglecting surface tension, the appropriate boundary conditions at the particle surface are continuity of velocity, normal stress, temperature, and heat flux. Assuming sufficiently small oscillations, see Sec. VII C, the boundary conditions are imposed at $r = a$,

$$v_{1r} = v'_{1r}, \quad v_{1\theta} = v'_{1\theta}, \quad T_1 = T'_1, \tag{54a}$$

$$\sigma_{1rr} = \sigma'_{1rr}, \quad \sigma_{1\theta r} = \sigma'_{1\theta r}, \quad k_{th}\partial_r T_1 = k'_{th}\partial_r T'_1. \tag{54b}$$

The boundary conditions are expressed in terms of the potentials using Eqs. (49), (50), and (52). The components of velocity and stress in spherical coordinates are given in Appendix A.

It is convenient to introduce the nondimensionalized wave numbers x_c, x_t, and x_s for the medium, and x'_c, x'_t, and x'_s for the particle:

$$x_c = k_c a, \quad x_t = k_t a, \quad x_s = k_s a, \tag{55a}$$

$$x'_c = k'_c a, \quad x'_t = k'_t a, \quad x'_s = k'_s a. \tag{55b}$$

Inserting the expansion (53) into the boundary conditions (54), and making use of the Legendre equation (C1), we obtain the following system of coupled linear equations for the expansion coefficients in each order n:

$\underline{a v_{1r} = a v'_{1r}}$

$$\begin{aligned} &x_c j'_n(x_c) + A_n x_c h'_n(x_c) + B_n x_t h'_n(x_t) - C_n n(n+1) h_n(x_s) \\ &= A'_n x'_c j'_n(x'_c) + B'_n x'_t j'_n(x'_t) - C'_n n(n+1) j_n(x'_s), \end{aligned} \tag{56a}$$

$\underline{a v_{1\theta} = a v'_{1\theta}}$

$$\begin{aligned} &j_n(x_c) + A_n h_n(x_c) + B_n h_n(x_t) - C_n[x_s h'_n(x_s) + h_n(x_s)] \\ &= A'_n j_n(x'_c) + B'_n j_n(x'_t) - C'_n[x'_s j'_n(x'_s) + j_n(x'_s)], \end{aligned} \tag{56b}$$

$\underline{T_1 = T'_1}$

$$\begin{aligned} &b_c j_n(x_c) + A_n b_c h_n(x_c) + B_n b_t h_n(x_t) \\ &= A'_n b'_c j_n(x'_c) + B'_n b'_t j_n(x'_t), \end{aligned} \tag{56c}$$

$\underline{a k_{th}\partial_r T_1 = a k'_{th}\partial_r T'_1}$

$$\begin{aligned} &k_{th} b_c x_c j'_n(x_c) + A_n k_{th} b_c x_c h'_n(x_c) + B_n k_{th} b_t x_t h'_n(x_t) \\ &= A'_n k'_{th} b'_c x'_c j'_n(x'_c) + B'_n k'_{th} b'_t x'_t j'_n(x'_t), \end{aligned} \tag{56d}$$

$\underline{a^2\sigma_{1\theta r} = a^2\sigma'_{1\theta r}}$

$$\begin{aligned} &\eta_0[x_c j''_n(x_c) - j_n(x_c)] + A_n\eta_0[x_c h''_n(x_c) - h_n(x_c)] \\ &\quad + B_n\eta_0[x_t h''_n(x_t) - h_n(x_t)] \\ &\quad - \frac{1}{2}C_n\eta_0\left[x_s^2 h''_n(x_s) + (n^2+n-2)h_n(x_s)\right] \\ &= A'_n\eta'_0[x'_c j''_n(x'_c) - j_n(x'_c)] + B'_n\eta'_0[x'_t j''_n(x'_t) - j_n(x'_t)] \\ &\quad - \frac{1}{2}C'_n\eta'_0\left[x'^2_s j''_n(x'_s) + (n^2+n-2)j_n(x'_s)\right], \end{aligned} \tag{56e}$$

$\underline{a^2\sigma_{1rr} = a^2\sigma'_{1rr}}$

$$\begin{aligned} &\eta_0\left[\left(x_s^2 - 2x_c^2\right)j_n(x_c) - 2x_c^2 j''_n(x_c)\right] \\ &\quad + A_n\eta_0\left[\left(x_s^2 - 2x_c^2\right)h_n(x_c) - 2x_c^2 h''_n(x_c)\right] \\ &\quad + B_n\eta_0\left[\left(x_s^2 - 2x_t^2\right)h_n(x_t) - 2x_t^2 h''_n(x_t)\right] \\ &\quad + 2n(n+1)C_n\eta_0[x_s h'_n(x_s) - h_n(x_s)] \\ &= A'_n\eta'_0\left[\left(x'^2_s - 2x'^2_c\right)j_n(x'_c) - 2x'^2_c j''_n(x'_c)\right] \\ &\quad + B'_n\eta'_0\left[\left(x'^2_s - 2x'^2_t\right)j_n(x'_t) - 2x'^2_t j''_n(x'_t)\right] \\ &\quad + 2n(n+1)C'_n\eta'_0[x'_s j'_n(x'_s) - j_n(x'_s)]. \end{aligned} \tag{56f}$$

Here, primes on spherical Bessel and Hankel functions indicate derivatives with respect to the argument. The equations are valid for both a fluid and a solid particle, with η'_0 being the viscosity for a fluid particle and the shear constant [Eq. (41a)] for a solid particle.

For $n = 0$, the boundary conditions for $v_{1\theta}$ and $\sigma_{1\theta r}$ are trivially satisfied because there is no angular dependence in

the zeroth-order Legendre polynomial, $P_0(\cos\theta) = 1$. Consequently, $\psi_s = 0$, and we are left with four equations with four unknowns, namely, Eqs. (56a), (56c), (56d), and (56f) with $C_0 = C_0' = 0$.

The linear system of equations (56) may be solved for each order n yielding the scattered field with increasing accuracy as higher-order multipoles are taken into account, an approach referred to within the field of ultrasound characterization of emulsions and suspensions as ECAH theory after Epstein and Carhart [30] and Allegra and Hawley [31]. However, care must be taken due to the system matrix often being ill conditioned [42].

The long-wavelength limit is characterized by the small dimensionless parameter ε, given by

$$\varepsilon = k_0 a = 2\pi \frac{a}{\lambda} \ll 1. \tag{57}$$

In this limit, the dominant contributions to the scattered field are due to the $n = 0$ monopole and the $n = 1$ dipole terms, both proportional to ε^3, while the contribution of the nth-order multipole for $n > 1$ is proportional to $\varepsilon^{2n+1} \ll \varepsilon^3$.

D. Monopole scattering coefficient

To obtain the monopole scattering coefficient f_0 in Eq. (5), we solve for the expansion coefficient A_0 in Eq. (56) and use the identity $f_0 = 3i\, x_c^{-3} A_0$. The f_n coefficients are traditionally used in studies of acoustic radiation force, while the A_n coefficients are used in general scattering theory.

The solution to the inhomogeneous system of linear equations for $n = 0$ involves straightforward but lengthy algebra presented in Appendix B 1. In Eq. (B8) is given the general analytical expression for f_0 in the long-wavelength limit valid for any particle. In the following, this expression is given in explicit, simplified, closed analytical form for a thermoviscous droplet and a thermoelastic particle, respectively.

1. *Thermoviscous droplet in a fluid*

For a thermoviscous droplet in a fluid in the long-wavelength limit, the particle radius a and the viscous and thermal boundary layers both inside (δ_s', δ_t') and outside (δ_s, δ_t) the fluid droplet are all much smaller than the acoustic wavelength λ, while nothing is assumed about the relative magnitudes of a, δ_s, δ_s', δ_t, and δ_t'. Thus, using the nondimensionalized wave numbers of Eq. (55) and $\varepsilon = k_0 a$, the long-wavelength limit is defined as

$$|x_c|^2, |x_c'|^2 \sim \varepsilon^2 \ll 1 \quad \text{and} \tag{58a}$$

$$|x_c|^2, |x_c'|^2 \sim \varepsilon^2 \ll |x_s|^2, |x_s'|^2, |x_t|^2, |x_t'|^2, \tag{58b}$$

which implies

$$\Gamma_s, \Gamma_t, \frac{|b_c|}{|b_t|}, \frac{|b_c'|}{|b_t|} \sim \varepsilon^2 \ll 1. \tag{58c}$$

To first order in ε, the analytical result for the monopole scattering coefficient f_0^{fl} obtained from Eq. (B8) is most conveniently written as

$$f_0^{\mathrm{fl}} = 1 - \tilde{\kappa}_s + 3(\gamma - 1)\left(1 - \frac{\tilde{\alpha}_p}{\tilde{\rho}_0 \tilde{c}_p}\right)^2 H(x_t, x_t'), \tag{59a}$$

$$H(x_t, x_t') = \frac{1}{x_t^2}\left[\frac{1}{1 - i x_t} - \frac{1}{\tilde{k}_{\mathrm{th}}} \frac{\tan x_t'}{\tan x_t' - x_t'}\right]^{-1}, \tag{59b}$$

where $H(x_t, x_t')$ is a function of the particle radius a through the nondimensionalized thermal wave numbers x_t and x_t'. Epstein and Carhart obtained a corresponding result for A_0 but with a sign error in the thermal correction term [30], while the result of Allegra and Hawley [31] is in agreement with what we present here. The factor $(\gamma - 1)$ quantifies the coupling between heat and the mechanical pressure waves. This factor is multiplied by $[1 - \tilde{\alpha}_p/(\tilde{\rho}_0 \tilde{c}_p)]^2$, where the quantity $\xi_p = \alpha_p/(\rho_0 c_p)$, with unit m^3/J, may be interpreted as an isobaric expansion coefficient per added heat unit. The thermal correction can only be nonzero if there is a contrast $\tilde{\xi}_p \neq 1$ in this parameter.

In the weak dissipative limit of small boundary layers the function $H(x_t, x_t')$ is expanded to first order in δ_t/a and δ_t'/a, and using $\tan(x_t') \simeq i$, we obtain

$$f_0^{\mathrm{fl}} = 1 - \tilde{\kappa}_s - \frac{3}{2}\frac{(1+i)(\gamma - 1)}{1 + \tilde{D}_{\mathrm{th}}^{1/2} \tilde{k}_{\mathrm{th}}^{-1}}\left(1 - \frac{\tilde{\alpha}_p}{\tilde{\rho}_0 \tilde{c}_p}\right)^2 \frac{\delta_t}{a}$$

(small-width boundary layers). (60)

In the limit of zero boundary-layer thickness $\delta_t/a \to 0$, the thermal correction vanishes, and we obtain

$$f_0^{\mathrm{fl}} = 1 - \tilde{\kappa}_s \quad \text{(zero-width boundary layers)}, \tag{61}$$

which is the well-known result for a compressible sphere in an ideal [3] or a viscous [29] fluid.

In the opposite limit of a point particle, $a/\delta_t, a/\delta_t' \to 0$, we find $H(x_t, x_t') = -(1/3)\tilde{\rho}_0 \tilde{c}_p$, yielding

$$f_0^{\mathrm{fl}} = 1 - \tilde{\kappa}_s - (\gamma - 1)\tilde{\rho}_0 \tilde{c}_p \left(1 - \frac{\tilde{\alpha}_p}{\tilde{\rho}_0 \tilde{c}_p}\right)^2$$

(point-particle limit). (62)

Since $\gamma > 1$, the correction from thermal effects in the point-particle limit is negative. This implies that the thermal correction enhances the magnitude of f_0^{fl} for acoustically soft particles ($\tilde{\kappa}_s > 1$), while it diminishes the magnitude and eventually may reverse the sign of f_0^{fl} for acoustically hard particles ($\tilde{\kappa}_s < 1$).

Importantly, an inspection of the point-particle limit [Eq. (62)] leads to two noteworthy conclusions not previously discussed in the literature. First, the thermal contribution to f_0^{fl} allows a sign change of the acoustic radiation force for different-sized but otherwise identical particles. Second, the thermal contribution may result in forces that are orders of magnitude larger than expected from both ideal [3] and viscous [29] theory. For example, $\tilde{\rho}_0 \gg 1$ for particles or droplets in gases leads to a thermal contribution to f_0^{fl} two orders of magnitude larger than $1 - \tilde{\kappa}_s$. These predictions are discussed in more detail in Sec. VIII.

2. *Thermoelastic particle in a fluid*

For a thermoelastic particle in a fluid, the long-wavelength limit differs from that of a thermoviscous droplet [Eq. (58)] by the shear mode describing a propagating wave and not a viscous boundary layer. The wavelength of this transverse shear wave is comparable to that of the longitudinal compressional wave, and in the long-wavelength limit both are assumed to be large,

$$|x_c|^2,|x_c'|^2,|x_s'|^2 \sim \varepsilon^2 \ll 1 \quad \text{and} \tag{63a}$$

$$|x_c|^2,|x_c'|^2,|x_s'|^2 \sim \varepsilon^2 \ll |x_s|^2,|x_t|^2,|x_t'|^2, \tag{63b}$$

which implies

$$\Gamma_s,\Gamma_t,\frac{1}{|\tilde\eta_0|},\frac{|b_c|}{|b_t|},\frac{|b_c'|}{|b_t|} \sim \varepsilon^2 \ll 1. \tag{63c}$$

To first order in ε, the result Eq. (B8) for f_0^{sl} may be simplified as outlined in Appendix B, and one obtains after some manipulation

$$f_0^{sl} = \frac{1-\tilde\kappa_s+3(\gamma-1)\left[\left(1-\frac{\tilde\alpha_p}{\tilde\rho_0\tilde c_p}\right)\left(1-\frac{\chi'\tilde\alpha_p}{\tilde\rho_0\tilde c_p}\right)-\frac{4}{3}\frac{\chi'\tilde\alpha_p\tilde\kappa_s}{\tilde c_p}\frac{c_T'^2}{c^2}\left(1-\frac{\tilde\alpha_p}{\tilde\rho_0\tilde c_p\tilde\kappa_s}\right)\right]H(x_t,x_t')}{1+4(\gamma-1)\frac{\chi'\tilde\alpha_p^2}{\tilde\rho_0\tilde c_p^2}\frac{c_T'^2}{c^2}H(x_t,x_t')}, \tag{64}$$

where the function $H(x_t,x_t')$ is still given by the expression in Eq. (59b) with x_t' being the nondimensionalized thermal wave number in the solid particle obtained from Eq. (48b). In the limit of a point particle, $a/\delta_t,a/\delta_t' \to 0$, we find

$$f_0^{sl} = \frac{1-\tilde\kappa_s-\frac{(\gamma-1)\tilde\rho_0\tilde c_p}{1-X'}\left[\left(1-\frac{\tilde\alpha_p}{\tilde\rho_0\tilde c_p}\right)\left(1-\frac{\chi'\tilde\alpha_p}{\tilde\rho_0\tilde c_p}\right)-\frac{4}{3}\frac{\chi'\tilde\alpha_p\tilde\kappa_s}{\tilde c_p}\frac{c_T'^2}{c^2}\left(1-\frac{\tilde\alpha_p}{\tilde\rho_0\tilde c_p\tilde\kappa_s}\right)\right]}{1-\frac{4}{3}\frac{\gamma-1}{1-X'}\frac{\chi'\tilde\alpha_p^2}{\tilde c_p}\frac{c_T'^2}{c^2}} \quad \text{(point-particle limit)}. \tag{65}$$

Remarkably, in the point-particle limit, f_0^{sl} and f_0^{fl} differ in general. However, as expected, letting $c_T' \to 0$ in Eq. (64), f_0^{sl} reduces to f_0^{fl} [Eq. (59)] for all particle sizes.

In the weak dissipative limit of small boundary layers, $\delta_t,\delta_t' \ll a$, the second term in the denominator of Eq. (64) is small for typical material parameters. An expansion in δ_t/a and δ_t'/a then yields in analogy with Eq. (60),

$$f_0^{sl} = 1-\tilde\kappa_s-\frac{3}{2}\frac{(1+i)(\gamma-1)}{1+(1-X')^{1/2}\tilde D_{th}^{1/2}\tilde k_{th}^{-1}} \times\left(1-\frac{\tilde\alpha_p}{\tilde\rho_0\tilde c_p}\right)^2\frac{\delta_t}{a} \quad \text{(small-width boundary layers)}, \tag{66}$$

simplified using Eq. (39e). In the limit $\delta_t/a \to 0$, the thermal correction term vanishes,

$$f_0^{sl} = 1-\tilde\kappa_s \quad \text{(zero-width boundary layers)}. \tag{67}$$

In this limit, where boundary-layer effects are negligible, f_0^{sl} and f_0^{fl} are identical and, as expected, equal to the ideal [3] and viscous [29] results.

E. Dipole scattering coefficient

To obtain the dipole scattering coefficient f_1 in Eq. (5), we solve for the expansion coefficient A_1 in Eq. (56) and use the identity $f_1 = -6i\,x_c^{-3}A_1$. In the long-wavelength limit, the terms involving the coefficients B_1 and B_1' are neglected to first order in ε. This reduces the system of equations (56) for $n=1$ from six to four equations with the unknowns A_1, A_1', C_1, and C_1'. In Appendix B 2 we solve explicitly for A_1. Physically, the smallness of the B_1 and B_1' terms means that thermal effects are negligible compared to viscous effects. This is consistent with the dipole mode describing the center-of-mass oscillations of the undeformed particle.

1. *Thermoviscous droplet in a fluid*

The analytical expression for A_1 in the long-wavelength limit for a thermoviscous droplet in a fluid, as defined in Eq. (58), is given in Eq. (B23) of Appendix B 2. This expression for A_1 was also obtained by Allegra and Hawley [31] and, with a minor misprint, by Epstein and Carhart [30] in their studies of sound attenuation in emulsions and suspensions. We write the result for the dipole scattering coefficient f_1 in a form more suitable for comparison to the theory of acoustic radiation forces as presented by Gorkov [3] and Settnes and Bruus [29],

$$f_1^{fl} = \frac{2(\tilde\rho_0-1)[1+F(x_s,x_s')-G(x_s)]}{(2\tilde\rho_0+1)[1+F(x_s,x_s')]-3G(x_s)}, \tag{68a}$$

$$G(x_s) = \frac{3}{x_s}\left(\frac{1}{x_s}-i\right), \tag{68b}$$

$$F(x_s,x_s') = \frac{1-ix_s}{2(1-\tilde\eta_0)+\frac{\tilde\eta_0 x_s'^2(\tan x_s'-x_s')}{(3-x_s'^2)\tan x_s'-3x_s'}}. \tag{68c}$$

Even though no thermal effects are present in f_1^{fl}, Eq. (68) is nevertheless an extension of the result by Settnes and Bruus [29], since we have taken into account a finite viscosity in the droplet entering through the parameters $\tilde\eta_0$ and x_s'. In the limit $\tilde\eta_0 \to \infty$ of infinite droplet viscosity, the function $F(x_s,x_s')$ tends to zero, and we recover the result for f_1 obtained in Ref. [29].

In the weak dissipative limit of small boundary layers, $\delta_s, \delta_s' \ll a$, the dipole scattering coefficient for the thermoviscous droplet reduces to

$$f_1^{\mathrm{fl}} = \frac{2(\tilde{\rho}_0 - 1)}{2\tilde{\rho}_0 + 1}\left[1 + \frac{3(1+i)}{1 + \tilde{\nu}_0^{1/2}\tilde{\eta}_0^{-1}}\frac{\tilde{\rho}_0 - 1}{2\tilde{\rho}_0 + 1}\frac{\delta_s}{a}\right] \quad \text{(small-width boundary layers).} \tag{69}$$

2. Thermoelastic particle in a fluid

In the long-wavelength limit Eq. (63) of a thermoelastic solid particle in a fluid, we obtain the result

$$f_1^{\mathrm{sl}} = \frac{2(\tilde{\rho}_0 - 1)[1 - G(x_s)]}{2\tilde{\rho}_0 + 1 - 3G(x_s)}, \tag{70}$$

with the function $G(x_s)$ given in Eq. (68). In this expression, the only particle-related parameters are density and radius, and it is identical to that derived by Settnes and Bruus [29], who included the same two parameters in their study of scattering from a compressible particle in a viscous fluid using asymptotic matching.

In the small-width boundary layer limit, $\delta_s \ll a$, the dipole scattering coefficient for the thermoelastic solid particle f_1^{sl} reduces to

$$f_1^{\mathrm{sl}} = \frac{2(\tilde{\rho}_0 - 1)}{2\tilde{\rho}_0 + 1}\left[1 + 3(1+i)\frac{\tilde{\rho}_0 - 1}{2\tilde{\rho}_0 + 1}\frac{\delta_s}{a}\right] \quad \text{(small-width boundary layers),} \tag{71}$$

which closely resembles Eq. (69) for f_1^{fl}.

3. Asymptotic limits

In the zero-width boundary layer limit, the dipole scattering coefficients f_1^{fl} and f_1^{sl} both reduce to the ideal-fluid expression [3],

$$f_1^{\mathrm{fl}} = f_1^{\mathrm{sl}} = \frac{2(\tilde{\rho}_0 - 1)}{2\tilde{\rho}_0 + 1} \quad \text{(zero-width boundary layers).} \tag{72}$$

In the opposite limit of a point particle, $F(x_s, x_s') = 1/(2 + 3\tilde{\eta}_0)$ is finite and the expression for f_0^{fl} and f_0^{sl} is dominated by the $G(x_s)$ terms, with both cases yielding the asymptotic result

$$f_1^{\mathrm{fl}} = f_1^{\mathrm{sl}} = \tfrac{2}{3}(\tilde{\rho}_0 - 1) \quad \text{(point-particle limit).} \tag{73}$$

It is remarkable that for small particles suspended in a gas where $\tilde{\rho}_0 \gg 1$, the value of f_1 in Eq. (73) is three to five orders of magnitude larger than the value $f_1 = 1$ predicted by ideal-fluid theory [3].

VII. RANGE OF VALIDITY

Before turning to experimentally relevant predictions derived from our theory, we discuss the range of validity of our results imposed by the three main assumptions: the time periodicity of the total acoustic fields, the perturbation expansion of the acoustic fields, and the restrictions associated with size, shape, and motion of the suspended particle.

A. Time periodicity

The first fundamental assumption in our theory is the restriction to time-periodic total acoustic fields, which was used to obtain Eq. (3) for the acoustic radiation force evaluated at the static far-field surface $\partial\Omega_1$. Given a time-harmonic incident field, as studied in this work, a violation of time periodicity can only be caused by a nonzero time-averaged drift of the suspended particle. Denoting the speed of this drift by $v_p(t)$, we consider first the case of a steady particle drift. The assumption of time periodicity is then a good approximation if the displacement $\Delta\ell$ is small compared to the particle radius a during one acoustic oscillation cycle $\tau = 2\pi/\omega$ used in the time averaging. A nonzero, acoustically induced particle drift speed v_p must be of second or higher order in $\varepsilon_{\mathrm{ac}}$, $v_p/c \sim \varepsilon_{\mathrm{ac}}^2$, as all first-order fields have a zero time average. Thus

$$\frac{\Delta\ell}{a} \simeq \frac{v_p\tau}{a} = \frac{2\pi v_p}{\omega a} = \frac{2\pi}{k_0 a}\frac{v_p}{c} = \frac{\lambda}{a}\varepsilon_{\mathrm{ac}}^2 \ll 1, \tag{74}$$

and time periodicity is approximately upheld for reasonably small perturbation strengths $\varepsilon_{\mathrm{ac}} \ll \sqrt{a/\lambda}$, which is not a severe restriction in practice. In a given experimental situation, it is also easy to check if a measured nonzero drift velocity fulfills $v_p\tau \ll a$.

In the case of an unsteady drift speed $v_p(t)$, the time-averaged rate of change of momentum $\langle \frac{d\boldsymbol{P}}{dt} \rangle$ in the fluid volume bounded by $\partial\Omega_1$ in Eq. (2) is nonzero, thus violating the assumption $\langle \frac{d\boldsymbol{P}}{dt} \rangle = \boldsymbol{0}$ leading to Eq. (3). Only the unsteady growth of the viscous boundary layer in the fluid surrounding the accelerating particle contributes to $\langle \frac{d\boldsymbol{P}}{dt} \rangle$, since equal amounts of momentum are fluxed into and out of the static fluid volume in the steady problem. For Eq. (3) to remain approximately valid, we must require $\langle \frac{d\boldsymbol{P}}{dt} \rangle$ to be much smaller than $\boldsymbol{F}^{\mathrm{rad}}$. To check this requirement, we consider a constant radiation force accelerating the particle. When including the added mass from the fluid, this leads to the well-known time scale τ_p for the acceleration,

$$\tau_p = \frac{2\tilde{\rho}_0 + 1}{9\pi}\frac{a^2}{\delta_s^2}\,\tau. \tag{75}$$

Thus, small particles ($a \ll \delta_s$) are accelerated to their steady velocity in a time scale much shorter than the acoustic oscillation period ($\tau_p \ll \tau$), while the opposite ($\tau_p \gg \tau$) is the case for large particles ($a \gg \delta_s$). The unsteady momentum transfer to the fluid bounded by $\partial\Omega_1$ is obtained from the unsteady part $F_{\mathrm{drag}}^{\mathrm{unst}}(t)$ of the drag force on the particle as $\langle \frac{dP}{dt} \rangle = \frac{1}{\tau}\int_0^\tau F_{\mathrm{drag}}^{\mathrm{unst}}(t)\,dt$. Using the explicit expression for $F_{\mathrm{drag}}(t)$ given in problems 7 and 8 in §24 of Ref. [43], we obtain to leading order

$$\frac{1}{F^{\mathrm{rad}}}\left\langle \frac{dP}{dt} \right\rangle = \begin{cases} \dfrac{4}{2\tilde{\rho}_0 + 1}\dfrac{\delta_s}{a} \ll 1, & \text{for } a \gg \delta_s, \\ \dfrac{2}{\pi}\dfrac{a}{\delta_s} \ll 1, & \text{for } a \ll \delta_s. \end{cases} \tag{76}$$

We conclude that $\langle \frac{dP}{dt} \rangle \ll F^{\mathrm{rad}}$ in both the large and small particle limits, and hence the assumption of Eq. (3) is fulfilled in those limits.

Considering typical microparticle acoustophoresis experiments, the unsteady acceleration takes place on a time

scale between micro- and milliseconds, much shorter than the time of a full trajectory. Typically, the unsteady part of the trajectory is not resolved and it is not important to the experimentally observed quasisteady particle trajectory. In acoustic levitation [25–28], where there is no drift, the assumption of time periodicity is exact. We conclude that the assumption of time periodicity is not restricting practical applications of our theory.

B. Perturbation expansion and linearity

The second fundamental assumption of our theory is the validity of the perturbation expansion, which requires the acoustic perturbation parameter $\varepsilon_{\mathrm{ac}}$ of Eq. (10) to be much smaller than unity. For applications in particle handling in acoustophoretic microchips [12,14], this constraint is not very restrictive because typical resonant acoustic energy densities of 100 J/m^3 result in $\varepsilon_{\mathrm{ac}} \sim 10^{-4}$.

Given the validity of the linear first-order equations, the solutions we have obtained for f_0 and f_1 based on the particular incident plane wave $\phi_{\mathrm{i}} = \phi_0\, e^{ik_{\mathrm{c}}z}$ are general, since any incident wave at frequency ω can be written as a superposition of plane waves.

C. Oscillations of the suspended particle

The third fundamental assumption of our theory is the assumption of small particle oscillation amplitudes, allowing the boundary conditions to be evaluated at the fixed interface position $r = a$. In general, the oscillation amplitudes must be small in comparison to all other length scales. For small particles, $a \ll \delta_{\mathrm{s}},\delta_{\mathrm{t}}$, the smallest length scale is set by the particle radius a. In the opposite limit of small boundary layers, $a \gg \delta_{\mathrm{s}},\delta_{\mathrm{t}}$, thermoviscous theory reduces to ideal-fluid theory, and the boundary-layer length scales drop out of the equations, again leading to the smallest relevant length scale being the particle radius a. The assumption of small particle oscillation amplitudes leads to physical constraints on the volume oscillations, Figs. 1(a) and 1(b), and the center-of-mass oscillations, Fig. 1(c), discussed in the following.

The volume oscillations of the particle are due to mechanical and thermal expansion. From the definition of the compressibility κ_s' and the volumetric thermal expansion coefficient α_p', we estimate the maximum relative change in particle radius $\Delta a/a$ to be

$$\frac{\Delta a}{a} \simeq \frac{\kappa_s'}{3} p_1 = \frac{\tilde{\kappa}_s}{3}\varepsilon_{\mathrm{ac}} \ll 1, \tag{77a}$$

$$\frac{\Delta a}{a} \simeq \frac{\alpha_p'}{3} T_1 \simeq \frac{1}{3}\,(\gamma-1)\tilde{\alpha}_p\varepsilon_{\mathrm{ac}} \ll 1. \tag{77b}$$

Here, we have used $\kappa_s p_1 = \varepsilon_{\mathrm{ac}}$ and $T_1 = \frac{(\gamma-1)\kappa_s}{\alpha_p} p_1$ obtained from Eq. (14) in the adiabatic limit $s_1 = 0$ combined with Eq. (16). Except for gas bubbles in liquids, for which $\tilde{\kappa}_s \gg 1$, these inequalities are always fulfilled for small perturbation parameters $\varepsilon_{\mathrm{ac}}$.

The velocity of the center-of-mass oscillations is found from Eq. (37) of Ref. [29] to be $v_{\mathrm{p}}^{\mathrm{osc}} = \frac{3}{2}\frac{f_1}{\tilde{\rho}_0-1} v_{\mathrm{in}}$. In the large-particle limit, f_1 is given by Eq. (72), which implies $0 < v_{\mathrm{p}}^{\mathrm{osc}} < 3v_{\mathrm{in}}$, where the lower and the upper limit is for $\tilde{\rho}_0 \gg 1$ and $\tilde{\rho}_0 \ll 1$, respectively. In the point-particle limit, Eq. (73), $v_{\mathrm{p}}^{\mathrm{osc}} = v_{\mathrm{in}}$ independent of $\tilde{\rho}_0$. The relative displacement amplitude $\Delta\ell/a$ is hence estimated as

$$\frac{\Delta\ell}{a} \simeq \frac{v_{\mathrm{p}}^{\mathrm{osc}}}{\omega a} \simeq \begin{cases} \dfrac{3}{2\tilde{\rho}_0+1}\dfrac{\lambda}{2\pi a}\varepsilon_{\mathrm{ac}} \ll 1, & \text{for } a \gg \delta_{\mathrm{s}}, \\ \dfrac{\lambda}{2\pi a}\varepsilon_{\mathrm{ac}} \ll 1, & \text{for } a \ll \delta_{\mathrm{s}}, \end{cases} \tag{78}$$

and thus the general requirement is that $\varepsilon_{\mathrm{ac}} \ll 2\pi a/\lambda$. For large particles in typical experiments, this restriction is not severe. However, for small particles it can be restrictive. For example, to obtain $\Delta\ell/a < 0.05$, we find for particles of radius $a = 100$ nm in water at 1 MHz and particles of radius $a = 1$ μm in air at 1 kHz, that $\varepsilon_{\mathrm{ac}} \lesssim 10^{-5}$ and $\varepsilon_{\mathrm{ac}} \lesssim 10^{-6}$, respectively.

VIII. MICROPARTICLES AND DROPLETS IN STANDING PLANE WAVES

The special case of a one-dimensional (1D) standing plane wave is widely used in practical applications of the acoustic radiation force in microchannel resonators [8–21] and acoustic levitators [25–28]. The many application examples as well as its relative simplicity make the 1D case an obvious and useful testing ground of our theory. In the following, we illustrate the main differences between our full thermoviscous treatment and the ideal-fluid or viscous-fluid models using the typical parameter values listed in Table II.

We consider a standing plane wave of the form $p_{\mathrm{in}} = p_{\mathrm{a}}\cos(k_0 y)$, $\boldsymbol{v}_{\mathrm{in}} = \frac{i}{\rho_0 c}\, p_{\mathrm{a}}\sin(k_0 y)\boldsymbol{e}_y$, with acoustic energy density $E_{\mathrm{ac}} = \frac{1}{4}\kappa_s p_{\mathrm{a}}^2 = \frac{1}{4}\rho_0 v_{\mathrm{a}}^2$, where p_{a} and v_{a} are the pressure and the velocity amplitude, respectively. Expression (5) for the radiation force then simplifies to

$$\boldsymbol{F}_{1\mathrm{D}}^{\mathrm{rad}} = 4\pi\ \Phi_{\mathrm{ac}} a^3 k_0 E_{\mathrm{ac}} \sin(2k_0 y)\boldsymbol{e}_y, \tag{79a}$$

$$\Phi_{\mathrm{ac}} = \tfrac{1}{3}\mathrm{Re}[f_0] + \tfrac{1}{2}\mathrm{Re}[f_1], \tag{79b}$$

where Φ_{ac} is the so-called acoustic contrast factor. The radiation force is thus proportional to Φ_{ac}, which contains the effects of thermoviscous scattering in f_0 and f_1. Note that for positive acoustic contrast factors, $\Phi_{\mathrm{ac}} > 0$, the force is directed towards the pressure nodes of the standing wave, while for negative acoustic contrast factors, $\Phi_{\mathrm{ac}} < 0$, it is directed towards the antinodes.

The acoustic contrast factor Φ_{ac} may be evaluated directly for an arbitrary particle size by using the expressions for the scattering coefficients, either f_0^{fl} and f_1^{fl} for a fluid droplet or f_0^{sl} and f_1^{sl} for a solid particle. For ease of comparison to the work of King [1], Yosioka and Kawasima [2], and Doinikov [4–6], we give the expression for the acoustic contrast factor $\Phi_{\mathrm{ac}}^{\mathrm{fl}}$ of a fluid droplet for small boundary layers and in the point-particle limit. In the small-width boundary layer limit one obtains

$$\Phi_{\mathrm{ac}}^{\mathrm{fl}} = \frac{1}{3}\left(\frac{5\tilde{\rho}_0-2}{2\tilde{\rho}_0+1} - \tilde{\kappa}_s\right) + \frac{3}{1+\tilde{\nu}_0^{1/2}\tilde{\eta}_0^{-1}}\left(\frac{\tilde{\rho}_0-1}{2\tilde{\rho}_0+1}\right)^2\frac{\delta_{\mathrm{s}}}{a} - \frac{1}{2}\frac{\gamma-1}{1+\tilde{D}_{\mathrm{th}}^{1/2}\tilde{k}_{\mathrm{th}}^{-1}}\left(1-\frac{\tilde{\alpha}_p}{\tilde{\rho}_0\tilde{c}_p}\right)^2\frac{\delta_{\mathrm{t}}}{a}$$

(small-width boundary layers). (80)

TABLE II. Material parameter values at ambient pressure 0.1 MPa and temperature 300 K used in this study, given for water (wa) [44–47], an average liquid food oil [48], air [49], and polystyrene (ps) [50–53]. Parameter values for water and oil at other temperatures are obtained from the fits in Refs. [44,48].

Parameter	Symbol	Value (wa)	Value (oil)	Value (air)	Value (ps)	Unit
Longitudinal speed of sound	c	1.502×10^3	1.445×10^3	3.474×10^2	2.40×10^3	$\mathrm{m\,s^{-1}}$
Transverse speed of sound	c_T				1.15×10^3	$\mathrm{m\,s^{-1}}$
Mass density	ρ_0	9.966×10^2	9.226×10^2	1.161×10^0	1.05×10^3	$\mathrm{kg\,m^{-3}}$
Compressibility	κ_s	4.451×10^{-10}	5.192×10^{-10}	7.137×10^{-6}	2.38×10^{-10}	$\mathrm{Pa^{-1}}$
Thermal expansion coefficient	α_p	2.748×10^{-4}	7.046×10^{-4}	3.345×10^{-3}	2.09×10^{-4}	$\mathrm{K^{-1}}$
Specific heat capacity	c_p	4.181×10^3	2.058×10^3	1.007×10^3	1.22×10^3	$\mathrm{J\,kg^{-1}K^{-1}}$
Heat capacity ratio	γ	1.012×10^0	1.151×10^0	1.402×10^0	1.04×10^0	1
Shear viscosity	η_0	8.538×10^{-4}	4.153×10^{-2}	1.854×10^{-5}		Pa s
Bulk viscosity[a]	η_0^b	2.4×10^{-3}	8.3×10^{-2}	1.1×10^{-5}		Pa s
Thermal conductivity	k_th	6.095×10^{-1}	1.660×10^{-1}	2.638×10^{-2}	1.54×10^{-1}	$\mathrm{W\,m^{-1}\,K^{-1}}$

[a]The bulk viscosity is negligible for scattering in the long-wavelength limit but has been included for completeness. Values for water, oil, and air are estimated from Refs. [54], [55], and [56], respectively. For oil, η_0^b is obtained from the attenuation constant α_0 at 298.15 K and 10 MHz [55] using $\alpha_0 = 2\pi^2 f^2/(\rho_0 c^3)[\eta_0^\mathrm{b} + (4/3)\eta_0 + (\gamma-1)k_\mathrm{th}/c_p]$.

The first term is the well-known result given by Yosioka and Kawasima [2], which reduces to that of King [1] for incompressible particles for which $\tilde{\kappa}_s = 0$. The second term is the viscous correction, which agrees with the result of Settnes and Bruus [29] for infinite particle viscosities, but extends it to finite particle viscosities. Note that the viscous correction yields a positive contribution to the acoustic contrast factor, while the thermal correction from the third term is negative. The result given in Eq. (80) is in agreement with the expression for the radiation force in a standing plane wave given by Doinikov [6] in the weak dissipative limit of small boundary layers. However, this is not seen without considerable effort combining and reducing a number of equations. Although we find Doinikov's approach rigorous, it lacks transparency and is difficult to apply with confidence.

In the point-particle limit of infinitely large boundary-layer thicknesses compared to the particle size, we obtain

$$\Phi_\mathrm{ac}^\mathrm{fl} = \frac{1}{3}\left[(1-\tilde{\kappa}_s) - (1-\tilde{\rho}_0) - (\gamma-1)\tilde{\rho}_0\tilde{c}_p\left(1-\frac{\tilde{\alpha}_p}{\tilde{\rho}_0\tilde{c}_p}\right)^2\right] \quad \text{(point-particle limit)}, \tag{81}$$

in agreement with the viscous result of Settnes and Bruus [29], when omitting the last term stemming from thermal effects. The result for $\Phi_\mathrm{ac}^\mathrm{fl}$ in Eq. (81) is written in a form which emphasizes how parameter contrasts between particle and fluid lead to scattering. As expected, for $\tilde{\kappa}_s = 1$ and $\tilde{\rho}_0 = 1$, the scattering due to compressibility and density (inertia) mechanisms vanishes. This is true for large particles [1–3,29], and it is reasonable that it remains true in the point-particle limit. The expressions for the acoustic radiation force on a point particle in a standing plane wave given by Doinikov [4–6] do not have this property, which is likely due to a sign error or a misprint in the term corresponding to our dipole scattering coefficient f_1 in the point-particle limit in Eq. (73), as was also suggested by Settnes and Bruus [29].

The small-width boundary layer limit and the point-particle limit are useful for analyzing consequences of thermoviscous scattering on the acoustic radiation force, but we emphasize that our theory is not restricted to these limits. In general, the scattering coefficients f_0 and f_1 are functions of the nondimensionalized wave numbers x_s, x_t, x_s', and x_t'. These may all be expressed in terms of the particle radius a normalized by the thickness of the viscous boundary layer in the medium δ_s,

$$x_\mathrm{s} = (1+i)\,\frac{a}{\delta_\mathrm{s}}, \qquad x_\mathrm{s}' = (1+i)\sqrt{\frac{\tilde{\rho}_0}{\tilde{\eta}_0}}\,\frac{a}{\delta_\mathrm{s}}, \tag{82a}$$

$$x_\mathrm{t} = (1+i)\sqrt{\mathrm{Pr}}\,\frac{a}{\delta_\mathrm{s}}, \quad x_\mathrm{t}' = \frac{(1+i)}{\sqrt{1-X'}}\sqrt{\frac{\mathrm{Pr}}{\tilde{D}_\mathrm{th}}}\,\frac{a}{\delta_\mathrm{s}} \tag{82b}$$

where we have used $\delta_\mathrm{s}' = \delta_\mathrm{s}\sqrt{\tilde{\eta}_0/\tilde{\rho}_0}$, $\delta_\mathrm{t} = \delta_\mathrm{s}\sqrt{1/\mathrm{Pr}}$, $\delta_\mathrm{t}' = \delta_\mathrm{s}\sqrt{[(1-X')\tilde{D}_\mathrm{th}]/\mathrm{Pr}}$, with $\mathrm{Pr} = \nu_0/D_\mathrm{th}$ being the Prandtl number of the fluid medium and X' set to zero for the fluid droplet case. Below, we investigate the thermoviscous effects on the acoustic radiation force by plotting the acoustic contrast factor Φ_ac as a function of δ_s/a, ranging from zero boundary-layer effects at $\delta_\mathrm{s}/a = 0$ to maximum effects in the limit $\delta_\mathrm{s}/a \to \infty$.

A. Oil droplets in water and water droplets in oil

We first consider the cases of water with a suspended oil droplet (wa-oil) and of oil with a suspended water droplet (oil-wa) using the parameters of a typical food oil given in Table II. Since the density contrast of water and oil is small, the dipole scattering with its viscous effects is small, while on the other hand the thermal effects in the monopole scattering are significant. This is clearly seen from Fig. 3, where the acoustic contrast factor Φ_ac is plotted for the two cases as a function of δ_s/a using ideal theory, viscous theory (obtained from our thermoviscous theory by setting $D_\mathrm{th} = 0$), and full thermoviscous theory. In Fig. 3, we see that for submicrometer droplets at MHz frequency the thermoviscous theory leads to corrections around 100% as compared to the ideal and the viscous theory, which manifestly demonstrates the importance of thermal effects in such systems.

We note from Fig. 3(a) that the acoustic contrast factor of oil droplets in water is negative, which means that oil droplets are focused at the pressure antinodes. Conversely, water droplets in oil are thus expected to be focused at the pressure nodes.

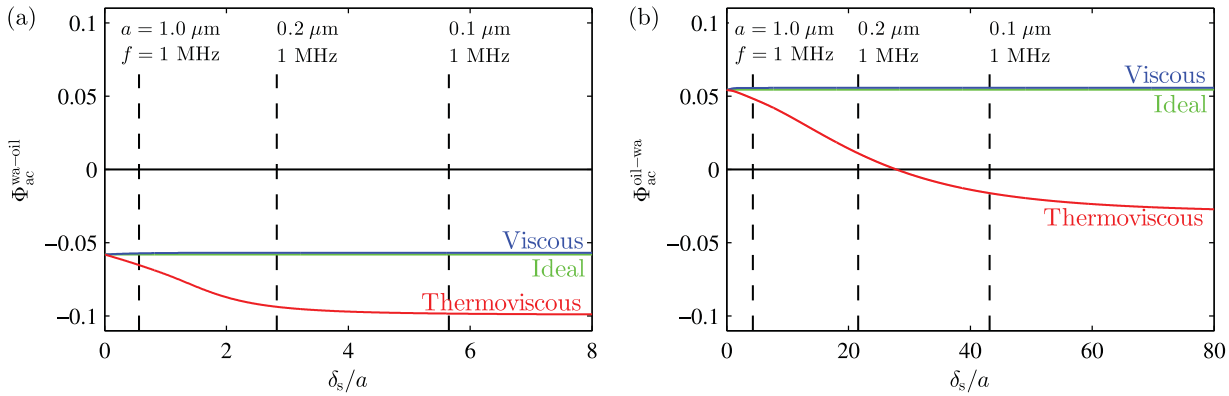

FIG. 3. (Color online) Acoustic contrast factor Φ_{ac} plotted as a function of δ_s/a, the viscous boundary-layer thickness in the medium normalized by particle radius. The curves are calculated using ideal theory (green), viscous theory (thermoviscous theory with $D_{th} = 0$, blue), and thermoviscous theory (red) for (a) an oil droplet in water (wa-oil) and (b) a water droplet in oil (oil-wa), both at 20 °C. Thermoviscous theory leads to corrections to the acoustic radiation force around 100%. The vertical dashed lines indicate examples of particle sizes corresponding to the given value of δ_s/a at $f = 1$ MHz. Note that the acoustic contrast factor changes sign at a critical particle radius for the case of water droplets in oil considered in (b).

However, in Fig. 3(b) we see that thermoviscous theory predicts a tunable sign change in the acoustic contrast factor as a result of the negative thermal corrections to the monopole scattering coefficient. This means that droplets above a critical size threshold experience a force directed towards the pressure nodes, while droplets smaller than the threshold experience a force towards the antinodes, even though the only distinction between the droplets is their size. This sign change in Φ_{ac} can also be achieved for elastic solid particles under properly tuned conditions. By changing, for example, the compressibility contrast $\tilde{\kappa}_s$, the curves for $\Phi_{ac}(\delta_s/a)$ may be shifted vertically and a possible size-threshold condition may be changed. Moreover, since $\delta_s = \sqrt{2\eta_0/(\rho_0\omega)}$ and $\delta_t = \sqrt{2k_{th}/(\rho_0 c_p \omega)}$, there are several direct ways of tuning a threshold value, e.g., by frequency or by changing the density of the medium.

B. Polystyrene particles and water droplets in air

Using the particular cases of a polystyrene particle and a water droplet suspended in air as main examples, we study the effects of a large density contrast $\tilde{\rho}_0 \gg 1$, for which our thermoviscous theory predicts much larger radiation forces on small particles than ideal-fluid theory, for which $\Phi_{ac}^{ideal} = 5/6$ independent of particle size. This is demonstrated in Fig. 4, where Φ_{ac} is plotted as a function of δ_s/a for the two particle types. In the large-particle limit $\delta_s/a = 0$, boundary-layer effects are negligible, and ideal, viscous ($D_{th} = 0$), and thermoviscous theories predict the same contrast factor $\Phi_{ac} = 5/6$, but as δ_s/a increases, the thermoviscous and viscous theories predict an increased value of Φ_{ac}, approximately $2\Phi_{ac}^{ideal}$ for $\delta_s/a = 1$ as seen in the insets of Figs. 4(a) and 4(b). Decreasing the particle size further, $\delta_s/a \gg 1$, the thermoviscous effects become more pronounced with $\Phi_{ac}/\Phi_{ac}^{ideal} \sim 10^2$. Choosing the frequency to be 1 kHz, this remarkable deviation from ideal-fluid theory is obtained for moderately-sized particles of radius $a \approx 2\,\mu$m.

While Φ_{ac}^{air-ps} in Fig. 4(a) for the polystyrene particle is a monotonically increasing function of δ_s/a, the Φ_{ac}^{air-wa} in Fig. 4(b) of a water droplet exhibits a nonmonotonic behavior. For small values of $\delta_s/a \lesssim 25$, the viscous dipole scattering dominates resulting in a positive contrast factor $\Phi_{ac}^{air-wa} \lesssim 10^2$. For larger values, $\delta_s/a \gtrsim 25$, thermal effects in the monopole scattering become dominant leading to a sign change in Φ_{ac}^{air-wa} and finally to large negative contrast factors approximately equal to -10^2 as the point-particle limit $\delta_s/a \gg 1$ is approached. This example clearly demonstrates how the acoustic contrast factor may exhibit a nontrivial size dependency with profound consequences for the acoustic radiation force on small particles. The detailed behavior depends on the specific materials but can be calculated using Eq. (79) and the expressions for f_0 and f_1 listed in Table I.

IX. CONCLUSION

Since the seminal work of Epstein and Carhart [30] and Allegra and Hawley [31], the effects of thermoviscous scattering have been known to be important for ultrasound attenuation in emulsions and suspensions of small particles. In this paper, we have by theoretical analysis shown that thermoviscous effects are equally important for the acoustic radiation force $\boldsymbol{F}^{rad}$ on a small particle. $\boldsymbol{F}^{rad}$ is evaluated from Eq. (5), or more generally from Eq. (6), using our analytical results for the thermoviscous scattering coefficients f_0 and f_1 summarized in Table I. Our analysis places no restrictions on the viscous and thermal boundary-layer thicknesses δ_s and δ_t relative to the particle radius a, a point which is essential to calculation of the acoustic radiation force on micrometer- and nanometer-sized particles.

The discussion in Sec. II leading to Eq. (5) for $\boldsymbol{F}^{rad}$ as well as the discussion of the range of validity presented in Sec. VII are intended to provide clarification and a deeper insight into the fundamental assumptions of the theory for the acoustic radiation force. Foremost, we have extended the discussions of the role of streaming, the fundamental assumption of time periodicity, and the trick of evaluating the radiation force in the far field, which led to the exact nonperturbative expression (3) for the radiation force evaluated in the far field.

For the simple case of a 1D standing plane wave at a single frequency, the expression (6) for $\boldsymbol{F}^{rad}$ simplifies to the useful expression given in Eq. (79), which involves the acoustic

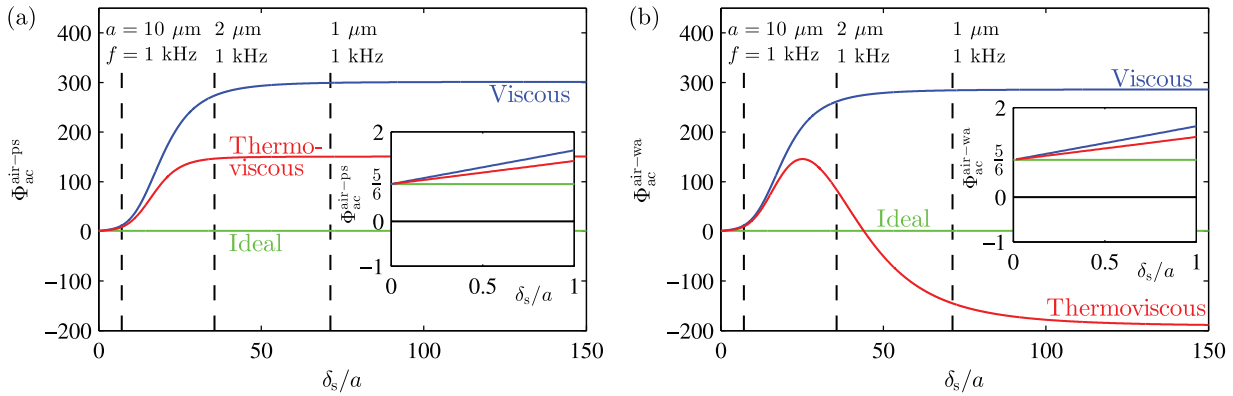

FIG. 4. (Color online) Acoustic contrast factor Φ_{ac} for particles in air plotted as a function of δ_s/a, the viscous boundary-layer thickness in the medium normalized by particle radius. The curves are calculated using ideal theory (green), viscous theory (thermoviscous theory with $D_{th} = 0$, blue), and thermoviscous theory (red) for (a) a polystyrene particle in air (air-ps) and (b) a water droplet in air (air-wa), both at 300 K. Ideal theory predicts a constant value of $\Phi_{ac} = 5/6$ independent of particle size. For particles much smaller than the boundary-layer thickness, however, thermoviscous theory predicts huge deviations from ideal theory leading to acoustic contrast factors two orders of magnitude larger than expected from ideal-fluid theory. The vertical dashed lines indicate examples of particle sizes corresponding to the given value of δ_s/a at $f = 1$ kHz.

contrast factor Φ_{ac}. Similar simplified expressions can be derived for other cases of interest such as that of a 1D traveling plane wave. An important result from the discussion of the simple 1D case in Sec. VIII is that we must abandon the notion of a purely material-dependent acoustic contrast factor Φ_{ac}. In general, Φ_{ac} also depends on the particle size, and in many cases this size dependency can even lead to a sign change in Φ_{ac} at a critical threshold. Recent acoustophoretic experiments on submicrometer-sized water droplets and smoke particles in air may provide the first evidence of this prediction [57]. Considering only viscous corrections, however, the authors could not fully explain their data. Our analysis suggests that thermoviscous effects must be taken into account when designing and analyzing such experiments.

Our results for the acoustic radiation force in a standing plane wave evaluated using Eq. (79) agree with the expressions obtained from the work of Doinikov [4–6] in the limit of small boundary layers, but not in the opposite limit of a point particle. In our theory both of these limits are evaluated directly using the derived analytical expressions valid for arbitrary boundary-layer thicknesses, and we have furthermore given a physical argument supporting our result in the point-particle limit. Considering the viscous theory of Danilov and Mironov [7], we remark that their result is based on the viscous reaction force on an oscillating rigid sphere [43] instead of a direct solution of the governing equations for an acoustic field scattering on a sphere.

Importantly, we have shown that the acoustic radiation force on a small particle including thermoviscous effects may deviate by orders of magnitude from the predictions of ideal-fluid theory when there is a large density contrast between the particle and the fluid. This result is particularly relevant for acoustic levitation and manipulation of small particles in gases [22–28]. Thermoviscous effects can also be significant in many lab-on-a-chip applications involving ultrasound handling of nanoparticles and nanodroplets. In general, acoustic boundary-layer effects should be expected for any type of submicrometer particle, including biological particles such as microvesicles, bacteria, and viruses [8,9,18]. A firm theoretical understanding of thermoviscous effects and of the particle-size-dependent sign change of the acoustic contrast factor could prove important for future applications relying on ultrasound manipulation of micrometer- and nanometer-sized particles.

APPENDIX A: VELOCITY AND NORMAL STRESS IN SPHERICAL COORDINATES

In spherical coordinates (r,θ,φ) with azimuthal symmetry, using that $\boldsymbol{v}_1 = \nabla\phi + \nabla\times\boldsymbol{\psi}$ with $\phi = \phi_c + \phi_t$ and $\boldsymbol{\psi} = \psi_s\,\boldsymbol{e}_\varphi$, the first-order velocity components are

$$v_{1r} = \partial_r\phi + \frac{1}{r\sin\theta}\partial_\theta[\sin\theta\ \psi_s], \tag{A1a}$$

$$v_{1\theta} = \frac{1}{r}\partial_\theta\phi - \frac{1}{r}\partial_r[r\ \psi_s]. \tag{A1b}$$

Inserting this into Eq. (52), we obtain the normal components of the first-order stress tensor

$$\sigma_{1rr} = \eta_0\left(2k_c^2 - k_s^2\right)\phi_c + \eta_0\left(2k_t^2 - k_s^2\right)\phi_t + 2\eta_0\partial_r^2\phi + \frac{2\eta_0}{\sin\theta}\partial_\theta\left[\sin\theta\left(\frac{1}{r}\partial_r\psi_s - \frac{1}{r^2}\psi_s\right)\right], \tag{A2a}$$

$$\sigma_{1\theta r} = 2\eta_0\partial_\theta\left(\frac{1}{r}\partial_r\phi - \frac{1}{r^2}\phi\right) - \eta_0\left(\partial_r^2\psi_s - \frac{2}{r^2}\psi_s\right) + \frac{\eta_0}{r^2}\partial_\theta\left[\frac{1}{\sin\theta}\partial_\theta(\sin\theta\ \psi_s)\right]. \tag{A2b}$$

APPENDIX B: SCATTERING COEFFICIENTS f_0 AND f_1

Here, we outline the calculation of the monopole and dipole scattering coefficients f_0 and f_1 in the long-wavelength limit where the particle radius and the boundary-layer thicknesses are assumed much smaller than the wavelength. Defining the small parameter $\varepsilon = k_0 a \ll 1$, we note that $k_0 a, k_0\delta_s, k_0\delta_t, k_0\delta_t'$, and for a fluid particle furthermore $k_0\delta_s'$, are all of order ε. The calculation is carried out to first order in ε.

1. Monopole scattering coefficient f_0

The monopole scattering coefficient f_0 may be obtained from Eqs. (56a), (56c), (56d), and (56f) setting $n = 0$ and $C_0 = C_0' = 0$. All Bessel functions of the small arguments $x_c, x_c' \sim \varepsilon \ll 1$ are expanded to first order in ε using Eq. (C5) of Appendix C, and in the (unprimed) fluid medium we neglect x_c^2 in comparison to x_s^2. Thus, we arrive at

$$A_0 \frac{i}{x_c} + A_0' \frac{1}{3} x_c'^2 - B_0 x_t h_1(x_t) + B_0' x_t' j_1(x_t') = \frac{1}{3} x_c^2, \tag{B1a}$$

$$A_0 b_c \left(1 - \frac{i}{x_c}\right) - A_0' b_c' + B_0 b_t h_0(x_t) - B_0' b_t' j_0(x_t') = -b_c, \tag{B1b}$$

$$A_0 k_{th} b_c \frac{i}{x_c} + A_0' \frac{1}{3} k_{th}' b_c' x_c'^2 - B_0 k_{th} b_t x_t h_1(x_t) + B_0' k_{th}' b_t' x_t' j_1(x_t') = \frac{1}{3} k_{th} b_c x_c^2, \tag{B1c}$$

$$\begin{aligned} &A_0 \eta_0 \left[\left(4 - x_s^2\right)\frac{i}{x_c} + x_s^2\right] - A_0' \eta_0' \left[x_s'^2 - \frac{4}{3} x_c'^2\right] + B_0 \eta_0 \left[\left(x_s^2 - 2x_t^2\right) h_0(x_t) - 2x_t^2 h_0''(x_t)\right] \\ &\quad - B_0' \eta_0' \left[\left(x_s'^2 - 2x_t'^2\right) j_0(x_t') - 2x_t'^2 j_0''(x_t')\right] = -\eta_0 x_s^2, \end{aligned} \tag{B1d}$$

where Eq. (C3) is used to write $g_0'(x) = -g_1(x)$ for any spherical Bessel or Hankel function $g_0(x)$.

Multiplying Eq. (B1c) by $1/(k_{th} b_t)$ and using the ratios

$$\frac{b_c}{b_t} = -(\gamma - 1)\frac{x_c^2}{x_t^2}, \quad \frac{b_c'}{b_c} = \tilde{\chi}\frac{\tilde{\alpha}_p}{\tilde{c}_p}, \quad \frac{b_t'}{b_t} = \frac{1}{\tilde{\chi}\tilde{\alpha}_p \tilde{D}_{th}}, \quad \frac{b_c'}{b_t} = \frac{b_c}{b_t}\frac{b_c'}{b_c} = -\tilde{\chi}(\gamma - 1)\frac{\tilde{\alpha}_p}{\tilde{c}_p}\frac{x_c^2}{x_t^2}, \tag{B2}$$

of the b coefficients defined in Eq. (50) [here, $\tilde{\chi} = 1$ for a droplet and $\tilde{\chi} = \chi'$ for a solid particle, respectively, while Eqs. (16), (22), and (39e) are used to reduce b_c'/b_c], we note that the A_0 and A_0' terms can be neglected to order ε, and we obtain

$$B_0' = \frac{k_{th} b_t}{k_{th}' b_t'} \frac{x_t h_1(x_t)}{x_t' j_1(x_t')} B_0 = \tilde{\chi}\frac{\tilde{\alpha}_p}{\tilde{\rho}_0 \tilde{c}_p} \frac{x_t h_1(x_t)}{x_t' j_1(x_t')} B_0. \tag{B3}$$

With this, we eliminate B_0' from the system of equations (B1), and the remaining three equations become

$$\begin{pmatrix} \frac{i}{x_c} & \frac{1}{3}x_c'^2 & -S_1 \\ \frac{b_c}{b_t}\left(\frac{i}{x_c} - 1\right) & \frac{b_c'}{b_t} & -\frac{S_2}{x_t^2} \\ \frac{i(x_s^2 - 4)}{x_c} - x_s^2 & \left(x_s'^2 - \frac{4}{3}x_c'^2\right)\tilde{\eta}_0 & -S_3 \end{pmatrix} \begin{pmatrix} A_0 \\ A_0' \\ B_0 \end{pmatrix} = \begin{pmatrix} \frac{x_c^2}{3} \\ \frac{b_c}{b_t} \\ x_s^2 \end{pmatrix}, \tag{B4}$$

where we have introduced the functions S_1, S_2, and S_3,

$$S_1 = \left[1 - \frac{1}{\tilde{k}_{th}}\frac{b_t}{b_t'}\right] x_t h_1(x_t), \tag{B5a}$$

$$S_2 = x_t^2 \left[\frac{h_0(x_t)}{x_t h_1(x_t)} - \frac{1}{\tilde{k}_{th}}\frac{j_0(x_t')}{x_t' j_1(x_t')}\right] x_t h_1(x_t), \tag{B5b}$$

$$S_3 = \left[\frac{x_s^2 h_0(x_t)}{x_t h_1(x_t)} - 4\left(1 - \frac{\tilde{\eta}_0}{\tilde{k}_{th}}\frac{b_t}{b_t'}\right) - \frac{\tilde{\eta}_0}{\tilde{k}_{th}}\frac{b_t x_s'^2}{b_t' x_t'}\frac{j_0(x_t')}{j_1(x_t')}\right] x_t h_1(x_t), \tag{B5c}$$

and the relative shear constant $\tilde{\eta}_0$ obtained from Eq. (41b),

$$\tilde{\eta}_0 = \frac{\eta_0'}{\eta_0} = \tilde{\rho}_0 \frac{x_s^2}{x_s'^2}. \tag{B6}$$

In obtaining the expression for S_3 we have used Eq. (C3) to substitute $g_0''(x) = -g_0(x) + (2/x)g_1(x)$ for any spherical Bessel or Hankel function $g(x)$. Using Eqs. (B2), (B6), and the explicit forms (C4) of the Bessel functions, the S functions are expressed

in terms of the dimensionless wave numbers as

$$S_1 = \left[1 - \tilde{\chi}\frac{\tilde{\alpha}_p}{\tilde{\rho}_0\tilde{c}_p}\right]x_\mathrm{t}h_1(x_\mathrm{t}), \tag{B7a}$$

$$S_2 = \frac{1}{H(x_\mathrm{t},x_\mathrm{t}')}\,x_\mathrm{t}h_1(x_\mathrm{t}), \tag{B7b}$$

$$S_3 = \left[\frac{x_\mathrm{s}^2}{1-ix_\mathrm{t}} - 4 + \frac{\tilde{\chi}\tilde{\alpha}_p}{\tilde{c}_p}\left(\frac{4x_\mathrm{s}^2}{x_\mathrm{s}'^2} - \frac{x_\mathrm{s}^2\tan x_\mathrm{t}'}{\tan x_\mathrm{t}' - x_\mathrm{t}'}\right)\right]x_\mathrm{t}h_1(x_\mathrm{t}), \tag{B7c}$$

where $H(x_\mathrm{t},x_\mathrm{t}')$ is given in Eq. (59b). The coefficient A_0 is now found from Eq. (B4) by the method of determinants (Cramer's rule) as $A_0 = D(A_0)/D$, where D is the determinant of the left-hand-side system matrix and $D(A_0)$ is the determinant of the system matrix in which the first column (the A_0 coefficients) are replaced by the right-hand-side column with the inhomogeneous terms. The monopole scattering coefficient f_0 in the long-wavelength limit can then be expressed as

$$f_0 = \frac{3i}{x_\mathrm{c}^3}\,A_0 = \frac{3i}{x_\mathrm{c}^3}\frac{D(A_0)}{D}, \tag{B8}$$

with the determinants D and $D(A_0)$ given by

$$\begin{aligned} D = -S_1\left[\tilde{\eta}_0\frac{b_\mathrm{c}}{b_\mathrm{t}}\left(\frac{i}{x_\mathrm{c}} - 1\right)\left(\frac{4}{3}x_\mathrm{c}'^2 - x_\mathrm{s}'^2\right) - \frac{b_\mathrm{c}'}{b_\mathrm{t}}\left(\left(4 - x_\mathrm{s}^2\right)\frac{i}{x_\mathrm{c}} + x_\mathrm{s}^2\right)\right] \\ - \frac{S_2}{x_\mathrm{t}^2}\left[\frac{x_\mathrm{c}'^2}{3}\left(\frac{i\left(4-x_\mathrm{s}^2\right)}{x_\mathrm{c}} + x_\mathrm{s}^2\right) - \frac{i\tilde{\eta}_0}{x_\mathrm{c}}\left(\frac{4}{3}x_\mathrm{c}'^2 - x_\mathrm{s}'^2\right)\right] - S_3\left[\frac{1}{3}x_\mathrm{c}'^2\frac{b_\mathrm{c}}{b_\mathrm{t}}\left(\frac{i}{x_\mathrm{c}} - 1\right) - \frac{i}{x_\mathrm{c}}\frac{b_\mathrm{c}'}{b_\mathrm{t}}\right], \end{aligned} \tag{B9a}$$

$$D(A_0) = -S_1\left[\tilde{\eta}_0\frac{b_\mathrm{c}}{b_\mathrm{t}}\left(\frac{4}{3}x_\mathrm{c}'^2 - x_\mathrm{s}'^2\right) + \frac{b_\mathrm{c}'}{b_\mathrm{t}}x_\mathrm{s}^2\right] - \frac{S_2}{3x_\mathrm{t}^2}\left[-\tilde{\eta}_0x_\mathrm{c}^2\left(\frac{4}{3}x_\mathrm{c}'^2 - x_\mathrm{s}'^2\right) - x_\mathrm{c}'^2x_\mathrm{s}^2\right] - \frac{S_3}{3}\left[\frac{b_\mathrm{c}}{b_\mathrm{t}}x_\mathrm{c}'^2 - \frac{b_\mathrm{c}'}{b_\mathrm{t}}x_\mathrm{c}^2\right]. \tag{B9b}$$

The solution $A_0 = D(A_0)/D$, though written somewhat differently, agrees with Allegra and Hawley's Eq. (10) of Ref. [31].

a. f_0 for a suspended thermoviscous droplet

For a suspended thermoviscous droplet, the precise definition of the long-wavelength limit is given in Eq. (58). In this case, the shear mode characterized by x_s' inside the droplet corresponds to a boundary layer, and consequently comparison to the compressional mode inside and outside the droplet yields $x_\mathrm{c}^2/x_\mathrm{s}'^2 \sim x_\mathrm{c}'^2/x_\mathrm{s}'^2 \sim \varepsilon^2 \ll 1$. This, combined with $b_\mathrm{c}/b_\mathrm{t} \sim b_\mathrm{c}'/b_\mathrm{t} \sim x_\mathrm{c}^2/x_\mathrm{t}^2 \sim \varepsilon^2 \ll 1$ from Eq. (B2), leads to the following simplification of Eq. (B9) to first order in ε,

$$D \simeq -\frac{i}{x_\mathrm{c}}\frac{x_\mathrm{s}^2}{x_\mathrm{t}^2}\tilde{\rho}_0S_2, \tag{B10a}$$

$$D(A_0) \simeq -\frac{\tilde{\rho}_0}{3}\frac{x_\mathrm{s}^2}{x_\mathrm{t}^2}\left(x_\mathrm{c}^2 - \frac{x_\mathrm{c}'^2}{\tilde{\rho}_0}\right)S_2 + \tilde{\rho}_0x_\mathrm{s}^2\frac{b_\mathrm{c}}{b_\mathrm{t}}\left(1 - \frac{\tilde{\alpha}_p}{\tilde{\rho}_0\tilde{c}_p}\right)S_1. \tag{B10b}$$

When inserting this into Eq. (B8), we obtain

$$f_0^\mathrm{fl} = 1 - \tilde{\kappa}_s + 3(\gamma - 1)\left(1 - \frac{\tilde{\alpha}_p}{\tilde{\rho}_0\tilde{c}_p}\right)\frac{S_1}{S_2}, \tag{B11}$$

which upon substitution with $\frac{S_1}{S_2} = (1 - \frac{\tilde{\alpha}_p}{\tilde{\rho}_0\tilde{c}_p})H(x_\mathrm{t},x_\mathrm{t}')$ from Eq. (B7) with $\tilde{\chi} = 1$, leads to the final analytical result for f_0^fl given in Eq. (59).

b. f_0 for a suspended thermoelastic particle

The qualitative change going from the thermoviscous droplet to the thermoelastic particle lies in the shear mode, which changes from a highly damped boundary-layer mode to a propagating transverse wave with $x_\mathrm{s}'^2 \sim \varepsilon^2$. A further implication is that the shear constant ratio of Eq. (B6) becomes large, $\tilde{\eta}_0 = \tilde{\rho}_0x_\mathrm{s}^2/x_\mathrm{s}'^2 \sim \varepsilon^{-2} \gg 1$; and the order of magnitude of the S functions of Eq. (B7) obey $S_1 \sim S_2 \sim \varepsilon^2S_3$. Combining this with the following expression derived from Eqs. (39e), (48), and (B6),

$$\tilde{\eta}_0\left(\frac{4}{3}x_\mathrm{c}'^2 - x_\mathrm{s}'^2\right) = -\chi'\tilde{\rho}_0x_\mathrm{s}^2, \tag{B12}$$

the leading-order expansions in ε of the determinants D and $D(A_0)$ in Eq. (B9) become

$$D = \frac{i}{x_c}\left(-\chi'\tilde{\rho}_0\frac{x_s^2}{x_t^2}S_2 + \frac{b_c'}{b_t}S_3\right), \tag{B13a}$$

$$D(A_0) = x_s^2\frac{b_c'}{b_t}\left(-1+\chi'\tilde{\rho}_0\frac{b_c}{b_c'}\right)S_1 + \frac{x_c^2}{3}\frac{x_s^2}{x_t^2}\left(\frac{x_c'^2}{x_c^2}-\chi'\tilde{\rho}_0\right)S_2 + \frac{x_c^2}{3}\frac{b_c'}{b_t}\left(1-\frac{b_c}{b_c'}\frac{x_c'^2}{x_c^2}\right)S_3. \tag{B13b}$$

From this and Eq. (B8), we obtain the monopole scattering coefficient $f_0^{\rm sl}$ for a thermoelastic particle suspended in a thermoviscous fluid,

$$f_0^{\rm sl} = \frac{3i}{x_c^3}A_0 = \frac{1-\frac{1}{\chi'\tilde{\rho}_0}\frac{x_c'^2}{x_c^2} - \frac{1}{\chi'\tilde{\rho}_0}\frac{b_c'}{b_t}\frac{x_t^2}{x_s^2}\left[\frac{3x_s^2}{x_c^2}\left(-1+\chi'\tilde{\rho}_0\frac{b_c}{b_c'}\right)\frac{S_1}{S_2} + \left(1-\frac{b_c}{b_c'}\frac{x_c'^2}{x_c^2}\right)\frac{S_3}{S_2}\right]}{1-\frac{1}{\chi'\tilde{\rho}_0}\frac{b_c'}{b_t}\frac{x_t^2}{x_s^2}\frac{S_3}{S_2}}. \tag{B14}$$

From Eq. (B7) we obtain the leading-order expansions in ε for the ratios S_1/S_2 and S_3/S_2,

$$\frac{S_1}{S_2} = \left(1-\frac{1}{\tilde{k}_{\rm th}}\frac{b_t}{b_t'}\right)H(x_t,x_t'), \quad \frac{S_3}{S_2} = 4\frac{\tilde{\eta}_0}{\tilde{k}_{\rm th}}\frac{b_t}{b_t'}H(x_t,x_t'), \tag{B15}$$

with the function $H(x_t,x_t')$ defined in Eq. (59b). Inserting this into Eq. (B14) and using Eqs. (B2) and (B6), and the expression (39e) for χ', we arrive at the final analytical form for $f_0^{\rm sl}$ given in Eq. (64).

2. Dipole scattering coefficient f_1

In the long-wavelength limit, for each order $n \geqslant 1$, the terms containing B_n and B_n', and thus the variables x_t and x_t', in the system of boundary equations (56) are of negligible order relative to the terms containing A_n, A_n', C_n, C_n', and the inhomogeneous terms. Formally, this is seen by writing up and inverting the entire 6-by-6 matrix equation for the six coefficients for a given $n \geqslant 1$. A quicker way to see this is to write Eqs. (56c) and (56d) as

$$\begin{pmatrix} h_n(x_t) & -j_n(x_t') \\ x_t h_n'(x_t) & -x_t' j_n'(x_t') \end{pmatrix}\begin{pmatrix} B_n \\ B_n' \end{pmatrix} \sim \varepsilon^2\begin{pmatrix} A_n' j_n(x_t') - A_n h_n(x_c) - j_n(x_c) \\ A_n' j_n(x_t') - A_n h_n(x_c) - j_n(x_c) \end{pmatrix}, \tag{B16}$$

where we have used $\frac{b_c}{b_t}, \frac{b_c'}{b_t} \sim \varepsilon^2$ and $\frac{b_t'}{b_t}, \frac{k_{\rm th}'}{k_{\rm th}} \sim 1$. Inserting the expressions for B_n and B_n' obtained by inversion of this equation into Eqs. (56a), (56b), (56e), and (56f), we see that due to the factor ε^2 all terms related to B_n or B_n' are negligible in all four equations. In treating Eq. (56e) it might be useful to use the Bessel's equation (C2). Consequently, returning to the dipole problem with $n = 1$, terms with B_1, B_1' are omitted and the system of equations reduces to four equations with four unknowns, namely, Eqs. (56a), (56b), (56e), and (56f) without the terms of B_1, B_1'. For $n = 1$ we thus obtain the simplified system of equations

$$x_c j_1'(x_c) + A_1 x_c h_1'(x_c) - 2C_1 h_1(x_s) = A_1' x_c' j_1'(x_c') - 2C_1' j_1(x_s'), \tag{B17a}$$

$$j_1(x_c) + A_1 h_1(x_c) - C_1[x_s h_1'(x_s) + h_1(x_s)] = A_1' j_1(x_c') - C_1'[x_s' j_1'(x_s') + j_1(x_s')], \tag{B17b}$$

$$\eta_0\left[x_c j_2(x_c) + A_1 x_c h_2(x_c) + \tfrac{1}{2}C_1 x_s^2 h_1''(x_s)\right] = \eta_0'\left[A_1' x_c' j_2(x_c') + \tfrac{1}{2}C_1' x_s'^2 j_1''(x_s')\right], \tag{B17c}$$

$$\eta_0\left[x_s^2 j_1(x_c) - 4x_c j_2(x_c)\right] - 4C_1\eta_0 x_s h_2(x_s) + A_1\eta_0\left[x_s^2 h_1(x_c) - 4x_c h_2(x_c)\right] = A_1'\eta_0'\left[x_s'^2 j_1(x_c') - 4x_c' j_2(x_c')\right] - 4C_1'\eta_0' x_s' j_2(x_s'), \tag{B17d}$$

where we have rewritten the last two equations using the recurrence relations obtained from Eq. (C3)

$$x g_1'(x) - g_1(x) = -x g_2(x), \tag{B18a}$$

$$g_1''(x) = -g_1(x) + \frac{2}{x}g_2(x), \tag{B18b}$$

valid for any spherical Bessel or Hankel function g.

Simplifying the system of equations we multiply Eq. (B17a) by (-1) and add to it Eq. (B17b), then use the recurrence relation (B18a). Equation (B17b) is multiplied by 2 and Eq. (B17a) is added while using the recurrence relation $x g_1'(x) + 2g_1(x) = x g_0(x)$. We leave Eq. (B17c) as it is. To Eq. (B17d) we add 4 times Eq. (B17c) and use the recurrence relation (B18b). With some

rearrangements, these manipulations give

$$A_1 x_c h_2(x_c) + C_1 x_s h_2(x_s) - A_1' x_c' j_2(x_c') - C_1' x_s' j_2(x_s') = -x_c j_2(x_c), \tag{B19a}$$

$$A_1 x_c h_0(x_c) - 2C_1 x_s h_0(x_s) - A_1' x_c' j_0(x_c') + 2C_1' x_s' j_0(x_s') = -x_c j_0(x_c), \tag{B19b}$$

$$A_1 x_c h_2(x_c) + \tfrac{1}{2} C_1 x_s^2 h_1''(x_s) - \tilde{\eta}_0 \big[A_1' x_c' j_2(x_c') + \tfrac{1}{2} C_1' x_s'^2 j_1''(x_s')\big] = -x_c j_2(x_c), \tag{B19c}$$

$$A_1 h_1(x_c) - 2C_1 h_1(x_s) - \tilde{\rho}_0 [A_1' j_1(x_c') - 2C_1' j_1(x_s')] = -j_1(x_c), \tag{B19d}$$

where $\tilde{\eta}_0 x_s'^2 = \tilde{\rho}_0 x_s^2$ was used to simplify the last equation. The equations may be further simplified using the relevant scalings in the long-wavelength limit for the fluid droplet and the solid particle, respectively.

a. f_1 for a suspended thermoviscous droplet

In the long-wavelength limit for the fluid droplet case the scalings of Eq. (58) apply. Using the approximate expressions for the spherical Bessel and Hankel functions [Eq. (C5)] applicable for small arguments and examining the resulting system of equations (B19) one finds that some terms may be omitted to first order in ε. The simplified system of equations (B19) for the fluid droplet case takes the form

$$-\frac{3i}{x_c^2} A_1 + C_1 x_s h_2(x_s) - C_1' x_s' j_2(x_s') = 0, \tag{B20a}$$

$$-2C_1 x_s h_0(x_s) - A_1' x_c' + 2C_1' x_s' j_0(x_s') = -x_c, \tag{B20b}$$

$$-\frac{3i}{x_c^2} A_1 + \frac{1}{2} C_1 x_s^2 h_1''(x_s) - \frac{1}{2} C_1' \tilde{\eta}_0 x_s'^2 j_1''(x_s') = 0, \tag{B20c}$$

$$\frac{3i}{x_c^2} A_1 + 6C_1 h_1(x_s) + A_1' \tilde{\rho}_0 x_c' - 6C_1' \tilde{\rho}_0 j_1(x_s') = x_c, \tag{B20d}$$

Subtracting Eq. (B20c) from Eq. (B20a) and using Eq. (B18b), we can express C_1' by C_1,

$$C_1' = \frac{x_s^2 h_1(x_s)}{\tilde{\eta}_0 x_s' Q(x_s')} C_1, \tag{B21a}$$

$$Q(x_s') = x_s' j_1(x_s') - 2\Big(1 - \tfrac{1}{\tilde{\eta}_0}\Big) j_2(x_s'). \tag{B21b}$$

Then, using this relation to eliminate C_1' in Eq. (B20a), we arrive at the first of the two equations in Eq. (B22). The second equation (B22b) is obtained by adding Eqs. (B20b) and (B20d) in order to eliminate A_1', then making use of the recurrence relation $3g_1(x) - x g_0(x) = x g_2(x)$. The resulting two equations for A_1 and C_1 are

$$\frac{3i}{x_c^2} A_1 - C_1 \left[x_s h_2(x_s) - \frac{x_s^2 h_1(x_s) j_2(x_s')}{\tilde{\eta}_0 Q(x_s')} \right] = 0, \tag{B22a}$$

$$\frac{3i}{x_c^2} A_1 + 2C_1 \tilde{\rho}_0 \left[\frac{3}{\tilde{\rho}_0} h_1(x_s) - x_s h_0(x_s) - \frac{x_s^2 h_1(x_s) j_2(x_s')}{\tilde{\eta}_0 Q(x_s')} \right] = (1 - \tilde{\rho}_0) x_c. \tag{B22b}$$

From this, and using again the relation $3g_1(x) - x g_0(x) = x g_2(x)$, we obtain the dipole expansion coefficient A_1,

$$A_1 = \frac{\frac{i}{3} x_c^3 (\tilde{\rho}_0 - 1)[h_2(x_s) \tilde{\eta}_0 Q(x_s') - x_s h_1(x_s) j_2(x_s')]}{[3h_2(x_s) - 2(\tilde{\rho}_0 - 1) h_0(x_s)] \tilde{\eta}_0 Q(x_s') - (2\tilde{\rho}_0 + 1) x_s h_1(x_s) j_2(x_s')}. \tag{B23}$$

This result, but with a small error in the numerator, was first obtained by Epstein and Carhart [30]. We reduce the fraction by $\tilde{\eta}_0 Q(x_s') h_0(x_s)$ and use the explicit expressions for the Bessel and Hankel functions in Eq. (C4) to introduce the functions $G(x_s)$ and $F(x_s, x_s')$ given explicitly in Eqs. (68b) and (68c), respectively,

$$G(x_s) = 1 + \frac{h_2(x_s)}{h_0(x_s)}, \tag{B24a}$$

$$F(x_s, x_s') = \frac{x_s h_1(x_s) j_2(x_s')}{\tilde{\eta}_0 h_0(x_s) Q(x_s')}. \tag{B24b}$$

Then, using that $f_1 = -6i\, x_c^{-3} A_1$, we arrive at the final expression (68a) for the dipole scattering coefficient f_1^{fl}.

b. f_1 for a suspended thermoelastic particle

In the long-wavelength limit for the solid particle the scalings of Eq. (63) apply. Using the approximate expressions for the spherical Bessel and Hankel functions [Eq. (C5)] applicable for small arguments and examining the resulting system of equations (B19) one finds that some terms may be omitted to first order in ε. The simplified system of equations (B19) in the solid particle case takes the form

$$-\frac{3i}{x_c^2}A_1 + C_1 x_s h_2(x_s) = 0, \tag{B25a}$$

$$-2C_1 x_s h_0(x_s) - A_1' x_c' + 2C_1' x_s' = -x_c, \tag{B25b}$$

$$-\frac{3i}{x_c^2}A_1 + \frac{1}{2}C_1 x_s^2 h_1''(x_s) - \frac{1}{15}A_1'\tilde{\eta}_0 x_c'^3 + \frac{1}{10}C_1'\tilde{\eta}_0 x_s'^3 = 0, \tag{B25c}$$

$$-\frac{3i}{x_c^2}A_1 - 6C_1 h_1(x_s) - A_1'\tilde{\rho}_0 x_c' + 2C_1'\tilde{\rho}_0 x_s' = -x_c, \tag{B25d}$$

Multiplying Eq. (B25b) by $(-\tilde{\rho}_0)$ and adding it to Eq. (B25d), then substituting C_1 using Eq. (B25a), and finally using the recurrence relation $3g_1(x) - xg_0(x) = xg_2(x)$ leads to the expansion coefficient A_1,

$$A_1 = \frac{\frac{i}{3}x_c^3(\tilde{\rho}_0 - 1)h_2(x_s)}{3h_2(x_s) - 2(\tilde{\rho}_0 - 1)h_0(x_s)}. \tag{B26}$$

Again, using that $f_1 = -6ix_c^{-3}A_1$ and introducing $G(x_s)$ as defined in Eq. (B24a), we obtain after some rearrangement the final result for f_1^{sl} given in Eq. (70).

APPENDIX C: SPECIAL FUNCTIONS

The Legendre differential equation solved by Legendre polynomials $P_n(\cos\theta)$ of order n is [58]

$$\frac{1}{\sin\theta}\frac{d}{d\theta}\left(\sin\theta\frac{d}{d\theta}P_n(\cos\theta)\right) + n(n+1)P_n(\cos\theta) = 0. \tag{C1}$$

The Bessel differential equation solved by spherical Bessel or Hankel functions $g_n(x)$ of order n is [58]

$$x^2[g_n''(x) + g_n(x)] = n(n+1)g_n(x) - 2xg_n'(x), \tag{C2}$$

with a prime indicating differentiation with respect to the argument. Useful recurrence relations for $g_n(x)$ are

$$\frac{d}{dx}[x^{-n}g_n(x)] = -x^{-n}g_{n+1}(x), \tag{C3a}$$

$$\frac{d}{dx}[x^{n+1}g_n(x)] = x^{n+1}g_{n-1}(x). \tag{C3b}$$

The lowest-order spherical Bessel functions $j_n(x)$ and Hankel functions of the first kind $h_n(x)$ are [58]

$$j_0(x) = \frac{\sin x}{x}, \quad j_1(x) = \frac{1}{x}\left(\frac{\sin x}{x} - \cos x\right), \tag{C4a}$$

$$j_2(x) = \frac{1}{x}\left[\left(\frac{3}{x^2} - 1\right)\sin x - \frac{3}{x}\cos x\right], \tag{C4b}$$

$$h_0(x) = -i\frac{e^{ix}}{x}, \quad h_1(x) = -\frac{e^{ix}}{x}\left(1 + \frac{i}{x}\right), \tag{C4c}$$

$$h_2(x) = i\frac{e^{ix}}{x}\left(1 + \frac{3i}{x} - \frac{3}{x^2}\right). \tag{C4d}$$

For small arguments, $x \ll 1$, to first order

$$j_0(x) \simeq 1, \quad j_0'(x) \simeq -\frac{x}{3}, \quad j_0''(x) \simeq -\frac{1}{3}, \tag{C5a}$$

$$h_0(x) \simeq 1 - \frac{i}{x}, \quad h_0'(x) \simeq \frac{i}{x^2}, \quad h_0''(x) \simeq -\frac{2i}{x^3}, \tag{C5b}$$

$$j_1(x) \simeq \frac{x}{3}, \quad j_2(x) \simeq \frac{x^2}{15}, \tag{C5c}$$

$$h_1(x) \simeq -\frac{i}{x^2}, \quad h_2(x) \simeq -\frac{3i}{x^3}. \tag{C5d}$$

[1] L. V. King, Proc. R. Soc. London, Ser. A **147**, 212 (1934).
[2] K. Yosioka and Y. Kawasima, Acustica **5**, 167 (1955).
[3] L. P. Gorkov, Sov. Phys. Dokl. **6**, 773 (1962) [Doklady Akademii Nauk SSSR **140**, 88 (1961)].
[4] A. A. Doinikov, J. Acoust. Soc. Am. **101**, 713 (1997).
[5] A. A. Doinikov, J. Acoust. Soc. Am. **101**, 722 (1997).
[6] A. A. Doinikov, J. Acoust. Soc. Am. **101**, 731 (1997).
[7] S. D. Danilov and M. A. Mironov, J. Acoust. Soc. Am. **107**, 143 (2000).
[8] B. Hammarström, T. Laurell, and J. Nilsson, Lab Chip **12**, 4296 (2012).
[9] M. Evander, O. Gidlof, B. Olde, D. Erlinge, and T. Laurell, Lab Chip **15**, 2588 (2015).
[10] I. Leibacher, P. Hahn, and J. Dual, Microfluid Nanofluid **19**, 923 (2015).
[11] H. Bruus, Lab Chip **11**, 3742 (2011).
[12] R. Barnkob, P. Augustsson, T. Laurell, and H. Bruus, Lab Chip **10**, 563 (2010).
[13] P. Thevoz, J. D. Adams, H. Shea, H. Bruus, and H. T. Soh, Anal. Chem. **82**, 3094 (2010).
[14] P. Augustsson, R. Barnkob, S. T. Wereley, H. Bruus, and T. Laurell, Lab Chip **11**, 4152 (2011).
[15] C. Grenvall, P. Augustsson, J. R. Folkenberg, and T. Laurell, Anal. Chem. **81**, 6195 (2009).
[16] Y. Liu, D. Hartono, and K.-M. Lim, Biomicrofluidics **6**, 012802 (2012).
[17] L. Schmid, D. A. Weitz, and T. Franke, Lab Chip **14**, 3710 (2014).
[18] M. Antfolk, P. B. Muller, P. Augustsson, H. Bruus, and T. Laurell, Lab Chip **14**, 2791 (2014).
[19] D. Carugo, T. Octon, W. Messaoudi, A. L. Fisher, M. Carboni, N. R. Harris, M. Hill, and P. Glynne-Jones, Lab Chip **14**, 3830 (2014).
[20] C. W. Shields, L. M. Johnson, L. Gao, and G. P. Lopez, Langmuir **30**, 3923 (2014).
[21] P. Li, Z. Mao, Z. Peng, L. Zhou, Y. Chen, P.-H. Huang, C. I. Truica, J. J. Drabick, W. S. El-Deiry, M. Dao, S. Suresh, and T. J. Huang, PNAS **112**, 4970 (2015).
[22] R. J. Imani and E. Robert, Ultrasonics **63**, 135 (2015).
[23] R. S. Budwig, M. J. Anderson, G. Putnam, and C. Manning, Ultrasonics **50**, 26 (2010).
[24] M. J. Anderson, R. S. Budwig, K. S. Line, and J. G. Frankel, Proc. IEEE Ultrasonics Symp. **1**, 481 (2002).
[25] E. H. Brandt, Nature **413**, 474 (2001).
[26] W. Xie and B. Wei, Appl. Phys. Lett. **79**, 881 (2001).
[27] V. Vandaele, P. Lambert, and A. Delchambre, Precis. Eng. **29**, 491 (2005).
[28] D. Foresti and D. Poulikakos, Phys. Rev. Lett. **112**, 024301 (2014).
[29] M. Settnes and H. Bruus, Phys. Rev. E **85**, 016327 (2012).
[30] P. S. Epstein and R. R. Carhart, J. Acoust. Soc. Am. **25**, 553 (1953).
[31] J. Allegra and S. Hawley, J. Acoust. Soc. Am. **51**, 1545 (1972).
[32] L. L. Foldy, Phys. Rev. **67**, 107 (1945).
[33] P. Lloyd and M. V. Berry, Proc. Phys. Soc. **91**, 678 (1967).
[34] D. J. McClements and M. J. W. Povey, J. Phys. D **22**, 38 (1989).
[35] R. E. Challis, M. J. W. Povey, M. L. Mather, and A. K. Holmes, Rep. Prog. Phys. **68**, 1541 (2005).
[36] P. B. Muller, R. Barnkob, M. J. H. Jensen, and H. Bruus, Lab Chip **12**, 4617 (2012).
[37] R. Barnkob, P. Augustsson, T. Laurell, and H. Bruus, Phys. Rev. E **86**, 056307 (2012).
[38] P. B. Muller, M. Rossi, A. G. Marin, R. Barnkob, P. Augustsson, T. Laurell, C. J. Kaehler, and H. Bruus, Phys. Rev. E **88**, 023006 (2013).
[39] H. Bruus, *Theoretical Microfluidics* (Oxford University Press, Oxford, 2008).
[40] L. D. Landau and E. M. Lifshitz, *Statistical Physics, Part 1*, 3rd ed., Vol. 5 (Butterworth-Heinemann, Oxford, 1980).
[41] L. D. Landau and E. M. Lifshitz, *Theory of Elasticity. Course of Theoretical Physics*, 3rd ed., Vol. 7 (Pergamon Press, Oxford, 1986).
[42] V. J. Pinfield, J. Acoust. Soc. Am. **122**, 205 (2007).
[43] L. D. Landau and E. M. Lifshitz, *Fluid Mechanics*, 2nd ed., Vol. 6 (Pergamon Press, Oxford, 1993).
[44] P. B. Muller and H. Bruus, Phys. Rev. E **90**, 043016 (2014).
[45] W. Wagner and A. Pruss, J. Phys. Chem. Ref. Data **31**, 387 (2002).
[46] M. L. Huber, R. A. Perkins, A. Laesecke, D. G. Friend, J. V. Sengers, M. J. Assael, I. N. Metaxa, E. Vogel, R. Mares, and K. Miyagawa, J. Phys. Chem. Ref. Data **38**, 101 (2009).
[47] M. L. Huber, R. A. Perkins, D. G. Friend, J. V. Sengers, M. J. Assael, I. N. Metaxa, K. Miyagawa, R. Hellmann, and E. Vogel, J. Phys. Chem. Ref. Data **41**, 033102 (2012).
[48] J. N. Coupland and D. J. McClements, J. Am. Oil Chem. Soc. **74**, 1559 (1997).
[49] *CRC Handbook of Chemistry and Physics*, 95th ed. (CRC Press, Boca Raton, FL, 2014).
[50] *Tables of Acoustic Properties of Materials: Plastics* (Onda Corporation, www.ondacorp.com/tecref_acoustictable.shtml, 2015).
[51] *CRC Polymers: A Properties Database* (CRC Press, Boca Raton, FL, 2014).
[52] E. S. Domalski and E. D. Hearing, J. Phys. Chem. Ref. Data **25**, 1 (1996).
[53] S. S. Chang and A. B. Bestul, J. Polym. Sci. A-2 Polym. Phys. **6**, 849 (1968).
[54] M. J. Holmes, N. G. Parker, and M. J. W. Povey, J. Phys. Conf. Ser. **269**, 012011 (2011).
[55] R. Chanamai and D. J. McClements, J. Am. Oil Chem. Soc. **75**, 1447 (1998).
[56] G. Prangsma, A. Alberga, and J. Beenakker, Physica **64**, 278 (1973).
[57] W. Ran and J. R. Saylor, J. Acoust. Soc. Am. **137**, 3288 (2015).
[58] G. B. Arfken and H. J. Weber, *Mathematical Methods for Physicists*, 6th ed. (Elsevier, New York, 2005).